Optimal digital filters for analyzing the mid-latency auditory P50 event-related potential in patients with Alzheimer's disease

Liljander, Sara

2016-06-15

Liljander , S , Holm , A , Keski-Säntti , P & Partanen , J V 2016 , ' Optimal digital filters for analyzing the mid-latency auditory P50 event-related potential in patients with Alzheimer's disease ' , Journal of Neuroscience Methods , vol. 266 , pp. 50-67 . https://doi.org/10.1016/j.jneumeth.2016.03.013

http://hdl.handle.net/10138/224052
https://doi.org/10.1016/j.jneumeth.2016.03.013

publishedVersion

Journal of Neuroscience Methods 266 (2016) 50–67

Contents lists available at ScienceDirect

Journal of Neuroscience Methods

journal homepage: www.elsevier.com/locate/jneumeth

Optimal digital filters for analyzing the mid-latency auditory P50 event-related potential in patients with Alzheimer's disease

Sara Liljander[a,*], Anu Holm[b], Petra Keski-Säntti[c], Juhani V. Partanen[a]

[a] Department of Clinical Neurophysiology, Jorvi Hospital, HUS Medical Imaging Center, Helsinki University Central Hospital, P.O. Box 800, FI-00029 HUS, Finland
[b] Department of Clinical Neurophysiology, Satakunta Central Hospital, Sairaalantie 3, FI-28500 Pori, Finland
[c] Department of Neurology, Jorvi Hospital, Helsinki University Central Hospital, P.O. Box 800, FI-00029 HUS, Finland

HIGHLIGHTS

- Filtering may severely distort the time-domain representations of ERP waveforms.
- Inappropriate filter parameters can lead to false conclusions.
- Careful filter design results in improved signal-to-noise ratio of ERP waveforms.
- The effect of different filter settings on the P50 component is investigated.
- The results provide evidence of optimal filters for P50 sensory gating analyses.

ARTICLE INFO

Article history:
Received 28 October 2015
Received in revised form 18 February 2016
Accepted 18 March 2016
Available online 22 March 2016

Keywords:
Event-related potential
P50
Sensory gating
Alzheimer's disease
Digital filter
Filter distortion

ABSTRACT

Background: Filtering is an effective pre-processing technique for improving the signal-to-noise ratio of ERP waveforms. Filters can, however, introduce substantial distortions into the time-domain representations of ERP waveforms. Inappropriate filter parameters may lead to the presence of statistically significant but artificial effects, whereas true effects may appear as insignificant.
New method: The present study aimed to determine the optimal digital filters for analyzing the auditory P50 component in patients with Alzheimer's disease. To provide evidence of the optimal filter settings, different high-pass and low-pass filters were applied to ERP waveforms obtained from a conditioning-testing paradigm. The results facilitate practical recommendations for selection of filters that maximize the signal-to-noise ratio of the P50 components without introducing significant distortions.
Results: The present study confirms that filter parameters have a significant effect on the amplitude and gating measures of the P50 component. Setting the high-pass cut-off at 0.1 Hz and the low-pass cut-off at 90 Hz (or above) is recommended for P50 component analyses.
Comparison with existing methods: The majority of ERP studies on sensory gating report using high-pass filters with 10-Hz cut-offs to measure P50 suppression. Such a high cut-off appeared to induce significant distortions into the ERP waveforms; thus, the authors advise against using these excessive high-pass cut-offs.
Conclusions: Filtering broadband signals, such as ERP signals, necessary results in time-domain distortions. However, by adjusting the filter parameters carefully according to the components of interest, it is possible to minimize filter artifacts and obtain more easily interpretable ERP waveforms.

1. Introduction

Sensory gating refers to the brain's ability to inhibit incoming repetitive and redundant sensory inputs (Braff and Geyer, 1990; Freedman et al., 1991; Light and Braff, 1999). Sensory gating is an essential neurocognitive function that protects the brain from sensory overload (Braff and Geyer, 1990; Light and Braff, 1999). Deficits in the sensory gating mechanism can lead to impairment of the

* Corresponding author. Tel.: +358 50 428 4308; fax: +358 9 471 85938.
E-mail addresses: sara.liljander@hus.fi, sara.liljander@gmail.com (S. Liljander), anu.holm@satadiag.fi (A. Holm), petra.keski-santti@terveystalo.com (P. Keski-Säntti), juhani.v.partanen@hus.fi (J.V. Partanen).

http://dx.doi.org/10.1016/j.jneumeth.2016.03.013
0165-0270/

brain's capacity to select, process, and store relevant information (Braff and Geyer, 1990).

Sensory gating can be measured via suppression of the mid-latency P50 component of the auditory event-related potential (ERP) (Adler et al., 1982; Boutros and Belger, 1999; Buchwald et al., 1989; Cancelli et al., 2006; Grunwald et al., 2003). The P50 component is a positive, small-amplitude response occurring about 50 ms after an auditory stimulus (Adler et al., 1982; Light and Braff, 1999). P50 suppression is considered to reflect automatic, pre-attentive processing of auditory information, in contrast to later, more elaborate processing (Boutros and Belger, 1999; Jerger et al., 1992; Wan et al., 2008).

In a conventional conditioning-testing paradigm, repeated pairs of identical auditory stimuli (usually clicks) are presented to assess P50 suppression (Adler et al., 1982; Braff and Geyer, 1990; Freedman et al., 1991; Light and Braff, 1999). The first stimulus (S1) activates an inhibitory response network while the shortly followed second stimulus (S2) tests the level of inhibition (Eccles, 1969; Light and Braff, 1999). The degree of P50 suppression is calculated as the gating ratio (S2/S1), i.e., the ratio of the P50 amplitude in response to the second stimulus (S2) relative to that of the first stimulus (S1) (Adler et al., 1982; Braff and Geyer, 1990; Freedman et al., 1991; Light and Braff, 1999), or as the gating difference (S1–S2), i.e., the P50 amplitude in response to the second stimulus (S2) subtracted from that of the first stimulus (S1) (Smith et al., 1994). Smaller S2/S1 ratios or larger S1–S2 differences indicate better inhibition, or "gating-out", of irrelevant sensory inputs (Boutros and Belger, 1999). In healthy subjects the P50 amplitude in response to the second stimulus is robustly suppressed, i.e., the amplitude to S2 is suppressed to 20–50% of the amplitude to S1 (Light and Braff, 1999).

Sensory gating has been investigated in a wide range of psychiatrically and neurologically impaired populations (Chang et al., 2012; Kisley et al., 2004; Light and Braff, 1999; Yadon et al., 2015). In contrast to a well-established sensory gating deficit in schizophrenia (Adler et al., 1982; Braff and Geyer, 1990; Freedman et al., 1991; Light and Braff, 1999), results on P50 suppression in patients with Alzheimer's disease have been contradictory (Ally et al., 2006; Cancelli et al., 2006; Fein et al., 1994; Jessen et al., 2001; Thomas et al., 2010). Since the mid-latency P50 component is highly sensitive to filter parameters (Chang et al., 2012; de Wilde et al., 2007; Freedman et al., 1998; Gmehlin et al., 2011; Jerger et al., 1992; Light and Braff, 1998; Patterson et al., 2008), in order to evaluate the validity of P50 as a biomarker for Alzheimer's disease, the effect of filtering on P50 sensory gating measures should be considered.

1.1. Digital filtering in the analysis of event-related potentials

Event-related potentials are embedded within the brain's spontaneous electrical activity (e.g., Luck, 2014). Compared to the ongoing background EEG from 10 to 100 μV in amplitude, the amplitude of electrical activity in response to stimulation is very small, ranging from 0.1 to 10 μV (Sörnmo and Laguna, 2005). To accurately extract ERP responses from the ongoing EEG and other signals considered as noise, various signal processing methods are applied (e.g., Acunzo et al., 2012; Luck, 2014; Picton et al., 1995).

Digital filtering is an effective pre-processing technique for improving the signal-to-noise ratio (Acunzo et al., 2012; Chang et al., 2012; Luck, 2014; Picton et al., 1995; Tanner et al., 2015; Widmann et al., 2015) and statistical power (Luck, 2014; Tanner et al., 2015) of ERP waveforms. Filters are used to attenuate frequency ranges that mainly contain signals of non-neural origin or irrelevant information in respect of the experimental effects being addressed (Acunzo et al., 2012; Luck, 2014; Tanner et al., 2015). Filtering can, however, significantly distort the time-domain representation of an ERP waveform, thus leading to false conclusions (Acunzo et al., 2012; Luck, 2014; Rousselet, 2012; Tanner et al., 2015; VanRullen, 2011; Widmann et al., 2015); filters may, e.g., alter the amplitude and timing of an ERP component (Luck, 2014; Tanner et al., 2015; VanRullen, 2011; Widmann and Schröger, 2012; Widmann et al., 2015) and introduce artificial peaks or oscillations (Luck, 2014; Tanner et al., 2015; Widmann et al., 2015). By assigning the filter parameters carefully according to the experimental design and components of interest, it is possible to minimize filter distortions and to detect small waveforms that without filtering would not be distinguishable from noise (Tanner et al., 2015; Widmann and Schröger, 2012; Widmann et al., 2015).

The most common types of digital filters in ERP research are low-pass and high-pass filters that selectively attenuate high-frequency and low-frequency components, respectively (e.g., Edgar et al., 2005; Luck, 2014; Tanner et al., 2015). The convolution property implies that the overall frequency response of two filters is equivalent to the product of the individual frequency responses (e.g., Luck, 2014, 2005); thus, a high-pass and a low-pass filter can be combined to form a band-pass filter that passes an intermediate range of frequencies (Edgar et al., 2005; Luck, 2014; Picton et al., 1995).

Low-pass filters are applied to eliminate high-frequency noise generated by external electrical devices (e.g., power-line noise at 50 or 60 Hz) or muscle activity (Luck, 2014). The contraction of muscles causes EMG artifacts that primarily consist of frequencies above 100 Hz; since frequencies above 100 Hz are often irrelevant in respect of cognitive responses, suppressing these relatively high frequencies with a low-pass filter will significantly reduce EMG artifacts while producing minimal distortion to the underlying ERP waveform (Luck, 2014; VanRullen, 2011).

In addition to suppressing high-frequency noise in the acquired EEG signals, it is often necessary to attenuate very low frequencies (Luck, 2014; Tanner et al., 2015). The objective of high-pass filtering is to remove slow voltage changes of non-neural origin caused by, e.g., skin potentials and movement artifacts (Luck, 2014). For a traditional ERP experiment, it is recommended to high-pass filter frequencies below approximately 0.1 Hz (Luck, 2014; Tanner et al., 2015). In less cooperative subjects (e.g., children and neurological patients) that are prone to head and body movements, a higher cut-off frequency, such as 0.5 or 1.0 Hz, might be of advantage (Luck, 2014). However, frequencies above 0.1 Hz may contribute essentially to the ERP waveform (Luck, 2014; Tanner et al., 2015): as the frequency content of the signal and the noise become more similar, suppression of the noise is likely to distort the signal (Luck, 2014). High-pass filters may also be useful for experiments that require dealing with overlapping activity from preceding and subsequent stimuli (Luck, 2005).

Sometimes ERP researchers use a notch filter to attenuate a narrow frequency band in the vicinity of 50 or 60 Hz power-line interference (e.g., Edgar et al., 2005; Luck, 2014). Notch filters can, however, introduce substantial distortions into the ERP waveform (Luck, 2005; Widmann et al., 2015); thus, application of a notch filter should be avoided, if possible. A notch filter may be replaced with a signal-processing technique utilizing a frequency-domain regression model with a Thompson *F*-test to adaptively estimate and remove sinusoidal noise (Mitra and Bokil, 2007) as, e.g., implemented in the CleanLine plugin for EEGLAB (Mullen, 2012).

1.2. Filter-induced distortions in ERP waveforms

Phase delay is a well-known filter distortion that shifts the frequency components of a signal forward in time (e.g., Acunzo et al., 2012; Luck, 2014; Widmann and Schröger, 2012; Widmann et al., 2015). Filters with a linear phase response delay all frequency components of an input signal by an equal amount of time points (e.g., Widmann et al., 2015). Linear-phase filters minimize filter-induced

distortions in the shape of an ERP waveform, but may generate large delays into the onset (Acunzo et al., 2012; Widmann et al., 2015). Nonlinear-phase filters delay different frequencies by different amounts of time (e.g., Widmann et al., 2015). Thus, filters with nonlinear phase may lead to severe distortions of the ERP waveform (Acunzo et al., 2012; Luck, 2014; Widmann et al., 2015).

Digital filters are classified as infinite impulse response (IIR) or finite impulse response (FIR) filters (e.g., Cook and Miller, 1992; Nitschke et al., 1998; Widmann et al., 2015). All IIR filters have a nonlinear phase response, whereas FIR filters can be designed to have either linear or nonlinear phase (e.g., Widmann et al., 2015). In comparison to FIR filters, IIR filters introduce less delay to the input signal (e.g., Acunzo et al., 2012) and are computationally more efficient as they require fewer coefficients (e.g., Acunzo et al., 2012; Widmann and Schröger, 2012; Widmann et al., 2015). FIR filters are always stable, whereas IIR filters can be unstable, are more difficult to control, and, due to the recursive structure of IIR filters, rounding errors can accumulate (e.g., Widmann and Schröger, 2012; Widmann et al., 2015).

Since the timing of cognitive processes is often of interest in ERP studies, phase shift is undesirable (Acunzo et al., 2012; Luck, 2014). Phase delay is characteristic of causal filters for which the output of the filter at a given time point depends on the past and present inputs but not on the future inputs (e.g., Acunzo et al., 2012; Luck, 2014; Widmann et al., 2015); i.e., the impulse response of a causal filter is zero prior to time zero (e.g., Luck, 2005; Rousselet, 2012). Both linear-phase and nonlinear-phase filters can be implemented as non-causal filters by filtering a signal twice, first in the forward direction and then in the backward direction (e.g., Acunzo et al., 2012; Rousselet, 2012; Widmann and Schröger, 2012); the impulse response of a non-causal filter is symmetric around time zero (e.g., Luck, 2014; Rousselet, 2012; Widmann et al., 2015). As a result, the non-causal filter has a zero-phase response, i.e., the filter introduces no phase delay (e.g., Acunzo et al., 2012; Rousselet, 2012; Widmann and Schröger, 2012; Widmann et al., 2015); the backward filtering counterbalances the delays introduced by forward filtering (e.g., Acunzo et al., 2012; Widmann et al., 2015). The two-pass filtering doubles the filter order and squares the magnitude response of the original filter (e.g., Widmann et al., 2015). A linear-phase filter can be implemented as a non-causal, zero-phase filter also by left-shifting the filter output by the filter's group delay (Widmann and Schröger, 2012; Widmann et al., 2015).

Since a non-causal filter has no phase delay, the filter does not shift peak latencies (Luck, 2014; Widmann et al., 2015). Instead, non-causal filters significantly distort the onset and offset latency of an ERP waveform, as well as the peak amplitudes (Luck, 2014; Rousselet, 2012; Tanner et al., 2015; VanRullen, 2011): the filtered waveform begins earlier and ends later than the unfiltered waveform. The spreading of an ERP waveform produced by non-causal low-pass filters is relatively modest (Luck, 2014; Rousselet, 2012) and typically has an equal effect on all subject groups and conditions in a given study (Luck, 2014); non-causal high-pass filters are more likely to introduce severe artificial effects (Luck, 2014; Rousselet, 2012; Tanner et al., 2015). Whereas the spreading of an ERP waveform introduced by low-pass filters is of the same polarity as the unfiltered waveform, high-pass filters produce artificial deflections of opposite polarity (Luck, 2014; Tanner et al., 2015). High-pass filters with sharp cut-offs may even induce artificial oscillations instead of single peaks before and after an elicited experimental effect (Luck, 2014; Tanner et al., 2015). The artificial peaks and oscillations produced by high-pass filters may lead an ERP researcher to draw spurious conclusions about which components are affected by a given experimental manipulation (Luck, 2005; Tanner et al., 2015).

ERP waveforms are typically comprised of small, high-frequency early components followed by larger, low-frequency late components (Luck, 2005). As a non-causal high-pass filter shifts low-frequency voltages forward and backward in time, the asymmetry of the sequence makes the induced bidirectional distortions particularly problematic; low-frequency information from the large-amplitude late components is shifted into the latency range of the early components, thus severely distorting the smaller early responses (Acunzo et al., 2012; Luck, 2005).

Distortions caused by non-causal high-pass filters may also lead to spurious conclusions in experiments where the difference between two ERP waveforms is investigated (Acunzo et al., 2012). When a non-causal filter is applied, the timing of the divergence between the two signals changes. Since differences in the later components distort the earlier components, artificial differences between the early responses that were not present in the original waveforms may be observed. If there is a difference between the non-causally filtered signals, the signals may only be stated to have a difference at some point in time, but this time point cannot be identified. With a causal filter the timing of the divergence of the two waveforms is preserved. Differences in the unfiltered waveforms may lead to differences at later time points but have no effect backward in time. The time point at which the causally filtered signals differed may be interpreted as the time point at which the original signals differed at the latest.

1.3. Selecting the filter type and parameters

Filters should not be used as a substitute for good data quality (Luck, 2014; Widmann et al., 2015); emphasis should be given to noise reduction at the source and a sufficient number of trials in the averages (Luck, 2014; Widmann and Schröger, 2012; Widmann et al., 2015). An analog low-pass filter is necessary during digitization in order to prevent aliasing (e.g., Edgar et al., 2005; Luck, 2014; Tanner et al., 2015), and some additional offline digital filtering is often required to accurately analyze ERP waveforms (Luck, 2014; Tanner et al., 2015; Widmann and Schröger, 2012; Widmann et al., 2015). Ubiquitously valid recommendations for selecting the optimal filters cannot be provided (Luck, 2014; Tanner et al., 2015; Widmann and Schröger, 2012; Widmann et al., 2015); the filter type and parameters need to be adjusted to meet the experimental question at hand. Almost without exception there is some degree of overlap in the frequency content of the ERP waveform and the noise to be filtered (Luck, 2005); thus, it is impossible to completely avoid filter artifacts (Luck, 2005; Tanner et al., 2015; Widmann et al., 2015). It is essential to understand the possible detriments caused by filtering and to select a filter with an optimal balance between noise reduction and distortion of the ERP waveform (Luck, 2014; Tanner et al., 2015; Widmann and Schröger, 2012; Widmann et al., 2015).

Precision in the time domain is inversely related to precision in the frequency domain (e.g., Cook and Miller, 1992; Edgar et al., 2005; Luck, 2014). Thus, using a filter to restrict frequency ranges in a signal necessarily results in temporal spreading of the waveform (Luck, 2014; Rousselet, 2012; Widmann and Schröger, 2012; Widmann et al., 2015). A sudden decline in the frequency response of a filter leads to a longer impulse response function with larger side-lobes (e.g., Luck, 2005; Rousselet, 2012); the steeper the transition band of a filter, the more the filtered waveform becomes spread out in time (Luck, 2005; Widmann et al., 2015). Since filtering can severely distort an ERP waveform, the signal should be filtered as little as possible (Luck, 2005; Rousselet, 2012). Filtering out very high and low frequencies may, however, drastically improve the signal-to-noise ratio of the ERP waveform (Luck, 2005; Widmann et al., 2015). Short filters with wide transition bands should be preferred to minimize temporal smearing and ringing artifacts (Luck, 2014; Widmann and Schröger, 2012; Widmann et al., 2015); this is a well-justified argument against using band-stop filters that require

an extremely steep roll-off (Widmann et al., 2015). The cut-off frequency and transition band of a filter should be separated from the frequency content of the ERP waveform in order to minimize filter distortions (Nitschke et al., 1998; Widmann and Schröger, 2012); therefore, filters with narrow transition bands may, however, be needed in experiments where the signal of interest and the noise to be removed consist of nearby frequency components (Cook and Miller, 1992; Edgar et al., 2005; Nitschke et al., 1998; Widmann et al., 2015). In high-pass filter design, the balance between the transition-band width and the cut-off frequency is particularly challenging, as on one hand the transition band is limited by DC, and on the other hand the cut-off frequency should be sufficiently low in order not to distort the slow components (Widmann and Schröger, 2012). The stop-band attenuation of a filter should be set only as high as necessary as it again requires a longer impulse response (Widmann and Schröger, 2012; Widmann et al., 2015).

Non-causal, zero-phase filters are recommended for the vast majority of ERP applications as they introduce no phase delay and thus minimize temporal distortion of the waveform (Luck, 2014; Widmann et al., 2015). A zero-phase filter is an appropriate choice for experiments where the timing of peaks is of interest (Acunzo et al., 2012). However, if the onset of an effect is to be investigated, a causal minimum-phase FIR filter is preferred for high-pass filtering (Widmann and Schröger, 2012); as a causal filter does not shift information back in time, a causal high-pass filter does not advance the onset of a waveform whereas a non-causal high-pass filter does (Luck, 2005; Rousselet, 2012; Widmann and Schröger, 2012). With a causal high-pass filter, the cut-off frequency may be set higher than with a non-causal filter, even at 2–5 Hz, to remove low-frequency noise without affecting the onset of a waveform (Rousselet, 2012). A causal low-pass filter introduces larger delays, even when converted to minimum-phase (Rousselet, 2012; Widmann et al., 2015); thus, causal low-pass filters are not recommended for ERP analyses (Widmann et al., 2015).

The convolution property implies that linear operations can be applied in any order (e.g., Luck, 2014, 2005). As signal averaging is also a linear operation, theoretically a digital filter can be applied either before or after averaging (Luck, 2014, 2005; Picton et al., 1995). As an averaged ERP waveform is smaller in data size, it would be computationally more efficient to filter the averaged waveform (Luck, 2005; Picton et al., 1995). Filtering may, however, produce edge artifacts at the beginning and end of a waveform (Luck, 2014; Tanner et al., 2015). The filtered value at a given time point is computed based on the surrounding time points; since some of these points may not exist near the beginning and end of the waveform, edge artifacts can occur. Therefore, filters should be applied on the continuous EEG prior to epoching or averaging in order for the filter to have a sufficiently long time series to operate properly (Luck, 2014; Tanner et al., 2015; Widmann et al., 2015). This is particularly an issue for high-pass filters with sharp cut-offs requiring a relatively long impulse response. Low-pass filters are less likely to produce significant edge artifacts, even when applied to epoched or averaged data (Luck, 2014; Tanner et al., 2015).

1.4. Filtering the mid-latency auditory P50 component

As the long-latency ERP components consist primarily of power below 30 Hz (Luck, 2005), a final band pass of approximately 0.1–30 Hz is recommended for traditional ERP experiments in cognitive neuroscience (Luck, 2014); the high-pass cut-off of 0.1 Hz effectively attenuates skin potentials and other slow voltage shifts, whereas the low-pass cut-off of 30 Hz filters out EMG activity and line noise. However, the choice of the appropriate cut-off frequency is dependent on the frequency content of the ERP components of interest and the noise to be filtered (Luck, 2005, 2014; Tanner et al., 2015).

The mid-latency auditory P50 component comprises mainly the brain's 40-Hz gamma activity (Başar et al., 1987; Brockhaus-Dumke et al., 2008; Gmehlin et al., 2011), thus requiring different filter settings than the analysis of the slow, long-latency ERP components (Gmehlin et al., 2011; Jerger et al., 1992). Despite the numerous studies addressing P50 sensory gating, literature does not provide rationalized guidelines for the selection of optimal filters for the analysis of the P50 component. The low-pass cut-offs vary greatly between studies, ranging from about 50 Hz to several hundred hertz (e.g., de Wilde et al., 2007; Freedman et al., 1998; Patterson et al., 2008). There is more consistency in the choice of the high-pass filter settings: the high-pass cut-offs typically range from DC to 10 Hz (e.g., de Wilde et al., 2007; Patterson et al., 2008), while the majority of studies report using a high-pass filter with a 10-Hz cut-off to measure P50 suppression (e.g., Brockhaus-Dumke et al., 2008; Chang et al., 2012; de Wilde et al., 2007; Freedman et al., 1998; Patterson et al., 2008). The excessive high-pass cut-offs are used to remove the influence of the large-amplitude N100 and P200 components on the small-amplitude P50 component (Ally et al., 2006; Cancelli et al., 2006; Jerger et al., 1992; Jessen et al., 2001). However, higher cut-off frequencies lead to greater distortions of the underlying ERP waveform, as more of the signal is attenuated by the filter (Luck, 2014; Tanner et al., 2015). Moreover, literature provides empirical evidence on how non-causal high-pass filters with cut-offs greater than 0.1 Hz can introduce artificial early ERP components, thus leading to false conclusions on which components are influenced by a given experimental manipulation (Acunzo et al., 2012). Consequently, the effects of filter settings and extreme high-pass cut-offs on the P50 component need to be better addressed.

The present study aimed to determine the optimal digital filters for analyzing the mid-latency auditory P50 component in patients with Alzheimer's disease. To evaluate the effects of filtering on the P50 component, different high-pass and low-pass filters were applied to ERP signals obtained from a passive conditioning-testing paradigm with the unfiltered ERP signals serving as a reference. Emphasis was given to demonstrate the consequences of the excessive high-pass cut-offs routinely used in the analysis of P50 sensory gating. Results provide empirical evidence for filter settings that optimize the signal-to-noise ratio of the P50 component without introducing significant distortions.

2. Materials and methods

2.1. Participants

Thirty-three patients diagnosed with Alzheimer's disease according to the Diagnostic and Statistical Manual of Mental Disorders, 4th Edition, Text Revision (DSM-IV-TR; American Psychiatric Association, 2000) participated in the study. The patients were recruited from the Department of Neurology in the Helsinki University Central Hospital. The study was approved by the Ethics Committee of the Helsinki and Uusimaa Hospital District, and a written informed consent was obtained from all participants. Five patients were excluded from analyses due to excessive artifacts (two due to 50-Hz line noise, three due to baseline drift), resulting in a final sample of 28 participants (mean age 70 years, range 57–78 years; 14 males, 14 females).

2.2. Stimuli and procedure

Instead of a typical paired-click paradigm, trains of four tones (frequency 1000 Hz, duration 60 ms, including a 10-ms rise and fall time) were delivered to both ears via headphones with an interstimulus interval (ISI) of 500 ms and an inter-trial interval (ITI) of 10 s. While the participants were watching a silent, attention-

Table 1
The parameters used in the filter design. The parameters in the table refer to the originally designed, one-pass filter (instead of the final, two-pass filter).

Half-amplitude cut-off f_c (−6 dB)	Hamming-windowed FIR		Least-square FIR		Butterworth 1st order IIR	Butterworth 2nd order IIR	Butterworth 3rd order IIR
	Transition-band width Δf	Filter order M	Transition-band width Δf	Filter order M	Half-power cut-off f_c (−3 dB)	Half-power cut-off f_c (−3 dB)	Half-power cut-off f_c (−3 dB)
0.1 Hz	0.2 Hz	8448	0.15 Hz	15360	0.17 Hz	0.13 Hz	0.12 Hz
0.5 Hz	1 Hz	1690	0.75 Hz	3072	0.87 Hz	0.66 Hz	0.60 Hz
1 Hz	2 Hz	846	1.5 Hz	1536	1.7 Hz	1.3 Hz	1.2 Hz
2 Hz	2 Hz	846	2 Hz	768	3.5 Hz	2.6 Hz	2.4 Hz
5 Hz	2 Hz	846	2 Hz	306	8.7 Hz	6.6 Hz	6.0 Hz
10 Hz	2.5 Hz	676	2.5 Hz	154	17.3 Hz	13.2 Hz	12.0 Hz
40 Hz	10 Hz	170	10 Hz	36	23.1 Hz	30.4 Hz	33.3 Hz
50 Hz	12.5 Hz	136	12.5 Hz	30	28.9 Hz	38.0 Hz	41.6 Hz
60 Hz	15 Hz	114	15 Hz	24	34.6 Hz	45.6 Hz	50.0 Hz
70 Hz	17.5 Hz	98	17.5 Hz	22	40.4 Hz	53.2 Hz	58.3 Hz
80 Hz	20 Hz	86	20 Hz	18	46.2 Hz	60.8 Hz	66.6 Hz
90 Hz	22.5 Hz	76	22.5 Hz	16	52.0 Hz	68.4 Hz	74.9 Hz

capturing movie, a set of 40 tone trains were presented with the stimulus intensity adjusted individually at 60 dB above the subjective hearing threshold. The participants were seated upright in a comfortable chair and instructed to remain relaxed, minimize movements, and ignore the sound stimuli.

2.3. Electrophysiological recordings

Recordings were performed with an EEG/ERP system Cognitrace (Version 3.3/4.0, eemagine Medical Imaging Solutions GmbH, Berlin, Germany). The EEG was recorded from 64 sintered Ag/AgCl electrodes embedded in an elastic cap (WaveGuard, eemagine Medical Imaging Solutions GmbH, Berlin, Germany) according to the extended 10–20 system. The EEG was referenced online to a common average reference. The electrocardiogram (ECG) was recorded bipolarly from electrodes placed below the right and left clavicle and the vertical electrooculogram (EOG) from electrodes placed above and below the left eye. The impedance was reduced to less than 10 kΩ at each electrode site. Signals were amplified with a Refa8-64 amplifier (TMS International, Enschede, The Netherlands), digitized at a sampling rate of 512 Hz to 22-bit accuracy, giving a resolution of 71.53 nV/bit (range ±150 mV), and filtered with a low-pass digital FIR filter with a cut-off frequency of 0.27 × sampling rate (i.e., 138.24 Hz). No high-pass filtering was applied during data acquisition (i.e., signals were direct coupled).

2.4. Digital filter design and implementation

All additional filtering was performed offline using MATLAB and Signal Processing Toolbox (Release 2014b, The MathWorks, Inc., Natick, MA) for digital-filter design and implementation. MATLAB toolbox EEGLAB (Version 13.4.4b; Delorme and Makeig, 2004) was utilized for importing the EEG signals into the MATLAB environment. To evaluate the effects of different filters on the P50 component, the filtering of the EEG signals was repeated with a Hamming-windowed FIR, least-square FIR, and Butterworth IIR filters. Each filter type was applied as a high-pass filter having a half-amplitude (−6 dB) cut-off at approximately 0.1 Hz, 0.5 Hz, 1 Hz, 2 Hz, 5 Hz, and 10 Hz, and as a low-pass filter having a half-amplitude cut-off at approximately 40 Hz, 50 Hz, 60 Hz, 70 Hz, 80 Hz, and 90 Hz. The high-pass and low-pass filters were applied independently on the continuous EEG, prior to epoching or averaging, in order to avoid edge artifacts.

The Signal Processing Toolbox function fir1 was used to design the Hamming-windowed sinc FIR filters. The function fir1 applies a window to the truncated inverse Fourier transform of an ideal, rectangular filter, i.e., the sinc-function (e.g., Widmann et al., 2015). The transition-band width (Δf) of the windowed FIR filters was designed to be twice the half-amplitude (−6 dB) cut-off (f_c), i.e., $\Delta f = 2 \times f_c$ for cut-offs $f_c \leq 1$ Hz, $\Delta f = 2$ Hz for cut-offs 1 Hz $< f_c \leq 8$ Hz, and $\Delta f = 0.25 \times f_c$ for cut-offs $f_c > 8$ Hz (after the EEGLAB default filter "*Basic FIR filter (new)*"; Table 1). As the transition-band width of a windowed sinc FIR filter is a function of filter order and window type, the required filter order with a Hamming window could be computed as $M = 3.3 \times (F_s/\Delta f)$ (e.g., Widmann et al., 2015), where F_s is the sampling frequency (512 Hz) and Δf the requested transition band. The computed filter order was rounded up to the nearest even integer to obtain an odd-length, symmetric (type I) linear-phase FIR filter (Table 1).

To design the least-square FIR filters, the function firls of the Signal Processing Toolbox was used. The function firls designs a linear-phase FIR filter that minimizes the integrated squared error between the magnitude response of the filter and the magnitude response of an ideal, rectangular filter over a set of desired frequency bands (Parks and Burrus, 1987). The transition-band width (Δf) of the least-square FIR filters was designed to be one and a half times the half-amplitude (−6 dB) cut-off (f_c), i.e., $\Delta f = 1.5 \times f_c$ for cut-offs $f_c \leq 1$ Hz, $\Delta f = 2$ Hz for cut-offs 1 Hz $< f_c \leq 8$ Hz, and $\Delta f = 0.25 \times f_c$ for cut-offs $f_c > 8$ Hz (Table 1). The filter order was computed as $M = 3 \times \mathrm{fix}(F_s/f_c)$ (after the EEGLAB filter "*Basic FIR filter (legacy)*"), where F_s is the sampling frequency and f_c the half-amplitude cut-off. The function fix rounds the quotient down to the nearest integer; if the computed filter order was odd-valued, it was incremented by one to obtain an odd-length, symmetric (type I) linear-phase FIR filter (Table 1).

The Butterworth IIR filters were designed using the function butter of the Signal Processing Toolbox. A Butterworth filter has a maximally flat frequency response in the pass band, i.e., the filter has no pass-band ripple, and has the shallowest roll-off near the cut-off frequency compared to other commonly used Chebyshev and elliptic IIR filters (e.g., Widmann et al., 2015). The roll-off rate of a Butterworth filter is −6 dB/octave per pole (or order). To examine the effect of the roll-off rate on the ERP waveforms, Butterworth filters of 1st, 2nd, and 3rd order were designed, having a roll-off of −6 dB/octave, −12 dB/octave, and −18 dB/octave, respectively. As the function butter returns the transfer function coefficients of a Nth-order digital Butterworth filter in terms of the half-power (−3 dB) cut-off frequency, the −3 dB cut-off of a filter with a specified −6 dB cut-off was approximated using the magnitude-squared response of an analog low-pass Butterworth filter: $|H_a(j\omega)|^2 = 1/(1 + (\omega/\omega_c)^{2N})$, where N is the filter order and ω_c the −3 dB cut-off angular frequency (e.g., Mitra, 2011). By substituting ω with the −6 dB cut-off angular frequency, the magnitude-squared response of a filter is given a value $|H_a(j\omega)|^2 = |1/2|^2$. As the angular frequency $\omega = 2\pi f$, the −3 dB cut-off frequency for a low-pass Butterworth filter could be computed

Table 2
The effect of different high-pass filters on the P50 amplitude (S1 amplitude) in response to the first stimulus sound (S1). The Wilcoxon signed-rank test with two-tailed exact significance was used to determine whether there was a statistically significant difference in the median S1 amplitude between the high-pass filtered and unfiltered waveforms. The median, first and third quartiles (Q1–Q3), and test statistics are reported for the S1 amplitude as a function of filter type and high-pass cut-off frequency. In the unfiltered waveforms the S1 amplitude was given a median of 4.63 μV (Q1–Q3 3.43–6.22 μV).

High-pass cut-off frequency	Filter type	S1 amplitude				
		Median (μV)	Q1–Q3 (μV)	Test statistics[a]		
				Z-score	*p*-value	Effect size *r*
0.1 Hz	Hamming-windowed FIR	4.69	3.36–5.90	−0.64[b]	0.53	−0.085
	Least-square FIR	4.69	3.35–5.89	−0.72[b]	0.48	−0.096
	Butterworth 1st order IIR	4.75	3.34–6.04	−0.63[c]	0.54	−0.084
	Butterworth 2nd order IIR	4.70	3.37–5.94	−0.51[b]	0.62	−0.068
	Butterworth 3rd order IIR	4.69	3.36–5.91	−0.65[b]	0.53	−0.087
0.5 Hz	Hamming-windowed FIR	4.97	3.15–6.10	−2.07[c]	**0.038**	−0.28
	Least-square FIR	4.94	3.17–6.15	−2.27[c]	**0.022**	−0.30*
	Butterworth 1st order IIR	5.18	3.58–6.31	−2.48[c]	**0.012**	−0.33*
	Butterworth 2nd order IIR	4.94	3.08–6.04	−1.66[c]	0.098	−0.22
	Butterworth 3rd order IIR	4.95	3.13–6.10	−2.04[c]	**0.041**	−0.27
1 Hz	Hamming-windowed FIR	4.84	3.28–6.03	−0.080[c]	0.94	−0.011
	Least-square FIR	4.85	3.26–6.09	−0.27[c]	0.79	−0.036
	Butterworth 1st order IIR	5.73	4.29–6.77	−3.60[c]	**<0.001**	−0.48*
	Butterworth 2nd order IIR	5.14	3.55–6.23	−1.11[c]	0.28	−0.15
	Butterworth 3rd order IIR	4.92	3.34–6.08	−0.44[c]	0.67	−0.059
2 Hz	Hamming-windowed FIR	5.32	3.71–6.63	−1.73[c]	0.085	−0.23
	Least-square FIR	5.32	3.70–6.62	−1.72[c]	0.087	−0.23
	Butterworth 1st order IIR	5.72	4.90–7.21	−3.68[c]	**<0.001**	−0.49*
	Butterworth 2nd order IIR	5.99	4.93–7.81	−4.29[c]	**<0.001**	−0.57**
	Butterworth 3rd order IIR	5.73	4.28–7.34	−3.62[c]	**<0.001**	−0.48**
5 Hz	Hamming-windowed FIR	8.14	6.82–10.30	−4.58[c]	**<0.001**	−0.61**
	Least-square FIR	7.81	6.74–9.96	−4.51[c]	**<0.001**	−0.60**
	Butterworth 1st order IIR	4.82	3.72–5.83	−0.44[b]	0.67	−0.059
	Butterworth 2nd order IIR	6.10	5.08–7.58	−3.01[c]	**0.002**	−0.40*
	Butterworth 3rd order IIR	6.70	5.77–8.58	−3.94[c]	**<0.001**	−0.53**
10 Hz	Hamming-windowed FIR	4.26	2.45–5.22	−2.15[b]	**0.030**	−0.29
	Least-square FIR	4.11	2.43–5.16	−2.37[b]	**0.017**	−0.32*
	Butterworth 1st order IIR	3.16	2.15–3.59	−4.03[b]	**<0.001**	−0.54**
	Butterworth 2nd order IIR	3.50	2.17–4.41	−3.33[b]	**<0.001**	−0.44*
	Butterworth 3rd order IIR	3.62	2.18–4.61	−3.03[b]	**0.002**	−0.40*

Note: [a] Wilcoxon signed-rank test; [b] based on positive ranks; [c] based on negative ranks; statistical significance ($\boldsymbol{p < 0.05}$) indicated in **bold**.
* Medium effect ($0.3 \leq |r| < 0.5$).
** Large effect ($|r| \geq 0.5$).

as f_c (−3 dB) = f_c (−6 dB)/$3^{1/(2N)}$ and for a high-pass Butterworth filter (replacing f_c with $1/f_c$) as f_c (−3 dB) = f_c (−6 dB) × $3^{1/(2N)}$ (Table 1).

Each filter was implemented as a non-causal, zero-phase filter using the Signal Processing Toolbox function filtfilt. The function filtfilt performs a bidirectional filtering by filtering the input signal both in the forward and reverse directions (e.g., Gustafsson, 1996; Widmann et al., 2015); as the two-pass filtering squares the magnitude response of the original filter, the −6 dB attenuation at the one-pass cut-off point is enhanced to −12 dB, along with doubling the originally defined filter order (e.g., Widmann et al., 2015).

2.5. Identification of the P50 component

Analyses of the ERP responses were conducted using software ASA (Version 4.8, eemagine Medical Imaging Solutions GmbH, Berlin, Germany). The EEG was re-referenced to the average of the left (M1) and right (M2) mastoid. No artifact rejection methods were applied, as without a reasonable band-pass filter baseline drift and other noise in the acquired EEG signals would have led to an unrepresentative sample of trials to be averaged. Moreover, no correction techniques were used for ocular artifacts as these artifacts were estimated to have a minor effect on the mid-latency P50 component: the potentials associated with blinks and saccades were estimated to have a lower frequency content than the P50 component (see Picton et al., 2000). The continuous EEG was segmented into epochs of 600 ms, starting 100 ms before and ending 500 ms after the onset of each stimulus. The epoched data were then averaged separately for the first, second, third, and fourth stimulus from each train at each electrode site. The averaged waveforms were baseline-corrected, with the mean voltage in the 100-ms prestimulus interval serving as a baseline. The single-subject averages were subsequently averaged for each filter setting to obtain the grand-averaged waveforms.

The P50 amplitude in response to the first and second stimulus (i.e., S1 amplitude and S2 amplitude, respectively) was further analyzed for each filter setting. As the P50 component was most prominent at the vertex, the amplitude measures were obtained at the Cz electrode site. The P50 component was identified as the most positive deflection within the time period of 30–70 ms post-stimulus. If two positive deflections were identified within that time period, i.e., P30 and P50, the latter deflection was taken as the P50. The peak amplitudes of the P50 component were measured relative to the pre-stimulus baseline using an automatic peak-detection algorithm. The automatically detected peaks were manually inspected and, if necessary, corrected; the averaged waveforms at two additional midline electrode sites, i.e., Fz and Pz, were utilized for the manual inspection. The gating ratio (S2/S1 ratio) was calculated as the P50 amplitude in response to the second stimulus (S2 amplitude) divided by the P50 amplitude in response to the first stimulus (S1 amplitude), i.e., (S2 amplitude)/(S1 amplitude). The gating difference (S1–S2 difference) was calculated as

Table 3
The effect of different high-pass filters on the P50 amplitude (S2 amplitude) in response to the second stimulus sound (S2). The Wilcoxon signed-rank test with two-tailed exact significance was used to determine whether there was a statistically significant difference in the median S2 amplitude between the high-pass filtered and unfiltered waveforms. The median, first and third quartiles (Q1–Q3), and test statistics are reported for the S2 amplitude as a function of filter type and high-pass cut-off frequency. In the unfiltered waveforms the S2 amplitude was given a median of 3.46 μV (Q1–Q3 2.52–4.46 μV).

High-pass cut-off frequency	Filter type	S2 amplitude				
		Median (μV)	Q1–Q3 (μV)	Test statistics[a]		
				Z-score	*p*-value	Effect size *r*
0.1 Hz	Hamming-windowed FIR	3.42	2.26–4.68	−0.83[b]	0.41	−0.11
	Least-square FIR	3.42	2.25–4.67	−0.98[b]	0.34	−0.13
	Butterworth 1st order IIR	3.43	2.41–4.73	−0.62[c]	0.55	−0.082
	Butterworth 2nd order IIR	3.42	2.28–4.71	−0.61[b]	0.55	−0.082
	Butterworth 3rd order IIR	3.42	2.26–4.69	−0.84[b]	0.41	−0.11
0.5 Hz	Hamming-windowed FIR	3.49	2.72–4.76	−2.87[c]	**0.003**	−0.38*
	Least-square FIR	3.50	2.71–4.80	−2.84[c]	**0.004**	−0.38*
	Butterworth 1st order IIR	3.65	2.84–4.81	−3.52[c]	**<0.001**	−0.47*
	Butterworth 2nd order IIR	3.54	2.77–4.79	−3.17[c]	**0.001**	−0.42*
	Butterworth 3rd order IIR	3.50	2.73–4.78	−2.90[c]	**0.003**	−0.39*
1 Hz	Hamming-windowed FIR	3.64	2.95–4.93	−3.82[c]	**<0.001**	−0.51**
	Least-square FIR	3.61	2.90–4.95	−3.60[c]	**<0.001**	−0.48*
	Butterworth 1st order IIR	3.85	3.10–4.82	−3.63[c]	**<0.001**	−0.49*
	Butterworth 2nd order IIR	3.73	2.95–4.87	−3.59[c]	**<0.001**	−0.48*
	Butterworth 3rd order IIR	3.62	2.93–4.91	−3.60[c]	**<0.001**	−0.48*
2 Hz	Hamming-windowed FIR	3.53	2.89–4.74	−2.16[c]	**0.030**	−0.29
	Least-square FIR	3.53	2.89–4.72	−2.16[c]	**0.029**	−0.29
	Butterworth 1st order IIR	3.94	3.31–4.79	−3.28[c]	**0.001**	−0.44*
	Butterworth 2nd order IIR	4.16	3.22–4.89	−3.59[c]	**<0.001**	−0.48*
	Butterworth 3rd order IIR	3.87	2.89–4.73	−2.66[c]	**0.006**	−0.36*
5 Hz	Hamming-windowed FIR	5.21	3.83–6.32	−4.08[c]	**<0.001**	−0.55**
	Least-square FIR	5.45	4.10–6.69	−4.30[c]	**<0.001**	−0.58**
	Butterworth 1st order IIR	3.10	2.70–3.84	−0.50[b]	0.63	−0.067
	Butterworth 2nd order IIR	4.16	3.38–5.30	−2.93[c]	**0.002**	−0.39*
	Butterworth 3rd order IIR	4.65	3.73–5.98	−3.83[c]	**<0.001**	−0.51**
10 Hz	Hamming-windowed FIR	2.66	2.15–3.66	−1.58[b]	0.12	−0.21
	Least-square FIR	2.68	2.10–3.54	−1.59[b]	0.11	−0.21
	Butterworth 1st order IIR	2.14	1.76–2.47	−3.17[b]	**0.001**	−0.42*
	Butterworth 2nd order IIR	2.43	1.90–2.94	−2.44[b]	**0.014**	−0.33
	Butterworth 3rd order IIR	2.63	1.89–3.12	−2.14[b]	**0.032**	−0.29

Note: [a] Wilcoxon signed-rank test; [b] based on positive ranks; [c] based on negative ranks; statistical significance (***p* < 0.05**) indicated in **bold**.
* Medium effect ($0.3 \leq |r| < 0.5$).
** Large effect ($|r| \geq 0.5$).

the P50 amplitude in response to the second stimulus (S2 amplitude) subtracted from the P50 amplitude in response to the first stimulus (S1 amplitude), i.e., (S1 amplitude)–(S2 amplitude).

2.6. Statistical analyses

Statistical analyses for the variables S1 amplitude, S2 amplitude, S2/S1 ratio, and S1–S2 difference were performed using IBM SPSS Statistics for Windows (Version 22.0, IBM Corp., Armonk, NY). The assumption of normality for the differences in the variables between the filtered and unfiltered waveforms was not satisfied for most of the filter settings, as assessed by the Shapiro–Wilk test ($p < 0.05$). Therefore, the non-parametric Wilcoxon signed-rank test with two-tailed exact significance was used to determine whether there was a statistically significant difference in the median of the variables between the filtered and unfiltered waveforms; the test was repeated for each filter setting. The level of significance was set at $\alpha = 0.05$. The effect sizes were calculated as the *Z*-score divided by the square root of the total sample size ($N = 56$) and classified as small ($|r| \geq 0.10$), medium ($|r| \geq 0.30$), or large ($|r| \geq 0.50$), according to Cohen's guidelines (Cohen, 1988).

3. Results

3.1. Filter responses

An example of the filter responses of the designed filters is shown in Fig. 1; the impulse, step, and magnitude responses are shown for high-pass filters with a 10-Hz cut-off (Fig. 1A–D) and low-pass filters with a 90-Hz cut-off (Fig. 1E–H). The shown filter responses refer to the final, two-pass filtering. The five different filter implementations resulted in notably deviant characteristics of the filters, despite the identical cut-off frequency.

The impulse and step responses give an impression of the time-domain distortions introduced by a filter (see also Rousselet, 2012; Widmann et al., 2015; Widmann and Schröger, 2012). The impulse response is the filter output in response to an impulse signal, whereas the step response reflects the filter output given an abrupt change in the input signal. As both impulse and step signals have power across the whole frequency spectrum, they provide practical evidence of the filter-induced distortions in spectrally complex or broadband signals, such as ERP waveforms (see also Widmann et al., 2015).

As shown by the impulse and step responses, both high-pass (Fig. 1A and B) and low-pass (Fig. 1E and F) filters cause temporal smearing of the input signal (see also Widmann et al., 2015). The step responses demonstrate the roughing effect of high-pass filters (Fig. 1B) and the smoothing effect of low-pass filters

Table 4
The effect of different high-pass filters on the P50 gating ratio (S2/S1 ratio), i.e., the ratio of the P50 amplitude in response to the second stimulus sound (S2) relative to that of the first stimulus sound (S1). The Wilcoxon signed-rank test with two-tailed exact significance was used to determine whether there was a statistically significant difference in the median S2/S1 ratio between the high-pass filtered and unfiltered waveforms. The median, first and third quartiles (Q1–Q3), and test statistics are reported for the S2/S1 ratio as a function of filter type and high-pass cut-off frequency. In the unfiltered waveforms the S2/S1 ratio was given a median of 0.66 (Q1–Q3 0.43–0.89).

High-pass cut-off frequency	Filter type	S2/S1 ratio				
		Median	Q1–Q3	Test statistics[a]		
				Z-score	*p*-value	Effect size *r*
0.1 Hz	Hamming-windowed FIR	0.65	0.42–0.89	−0.62[c]	0.55	−0.082
	Least-square FIR	0.65	0.42–0.89	−0.48[c]	0.65	−0.064
	Butterworth 1st order IIR	0.66	0.45–0.89	−1.89[c]	0.060	−0.25
	Butterworth 2nd order IIR	0.65	0.42–0.90	−0.65[c]	0.53	−0.087
	Butterworth 3rd order IIR	0.65	0.42–0.89	−0.59[c]	0.57	−0.079
0.5 Hz	Hamming-windowed FIR	0.68	0.55–0.87	−1.80[c]	0.074	−0.24
	Least-square FIR	0.67	0.54–0.88	−1.66[c]	0.10	−0.22
	Butterworth 1st order IIR	0.70	0.57–0.90	−2.26[c]	**0.023**	−0.30*
	Butterworth 2nd order IIR	0.71	0.55–0.89	−2.44[c]	**0.014**	−0.33*
	Butterworth 3rd order IIR	0.68	0.54–0.87	−1.98[c]	**0.048**	−0.26
1 Hz	Hamming-windowed FIR	0.76	0.60–1.03	−2.98[c]	**0.002**	−0.40*
	Least-square FIR	0.74	0.58–1.01	−2.85[c]	**0.003**	−0.38*
	Butterworth 1st order IIR	0.71	0.54–0.88	−0.62[c]	0.55	−0.082
	Butterworth 2nd order IIR	0.74	0.58–0.99	−2.76[c]	**0.005**	−0.37*
	Butterworth 3rd order IIR	0.75	0.59–1.01	−2.87[c]	**0.003**	−0.38*
2 Hz	Hamming-windowed FIR	0.72	0.48–0.92	−1.28[c]	0.21	−0.17
	Least-square FIR	0.72	0.48–0.92	−1.28[c]	0.21	−0.17
	Butterworth 1st order IIR	0.74	0.50–0.82	−0.091[b]	0.94	−0.012
	Butterworth 2nd order IIR	0.71	0.49–0.82	−0.52[b]	0.61	−0.070
	Butterworth 3rd order IIR	0.68	0.45–0.84	−0.39[b]	0.71	−0.052
5 Hz	Hamming-windowed FIR	0.62	0.54–0.75	−1.07[b]	0.29	−0.14
	Least-square FIR	0.69	0.60–0.81	−0.30[b]	0.78	−0.040
	Butterworth 1st order IIR	0.75	0.54–0.90	−0.64[c]	0.54	−0.085
	Butterworth 2nd order IIR	0.74	0.58–0.84	−0.36[c]	0.73	−0.049
	Butterworth 3rd order IIR	0.71	0.60–0.82	−0.36[c]	0.73	−0.049
10 Hz	Hamming-windowed FIR	0.76	0.56–1.08	−1.62[c]	0.11	−0.22
	Least-square FIR	0.78	0.57–1.10	−1.66[c]	0.10	−0.22
	Butterworth 1st order IIR	0.79	0.60–0.96	−1.39[c]	0.17	−0.19
	Butterworth 2nd order IIR	0.82	0.61–1.02	−1.44[c]	0.16	−0.19
	Butterworth 3rd order IIR	0.82	0.59–1.06	−1.55[c]	0.13	−0.21

Note: [a] Wilcoxon signed-rank test; [b] based on positive ranks; [c] based on negative ranks; statistical significance (***p* < 0.05**) indicated in **bold**.
* medium effect ($0.3 \leq |r| < 0.5$).

(Fig. 1F; see also Widmann et al., 2015). The step responses of the low-pass windowed FIR and least-square FIR filters exhibit a significant under/overshoot before and after the step (Fig. 1F); the under/overshoot is also apparent for the 2nd and 3rd order Butterworth filters but not for the 1st order Butterworth filter.

The magnitude response (along with the phase response) describes a filter in the frequency domain (see also Rousselet, 2012; Widmann et al., 2015; Widmann and Schröger, 2012). Due to the small values of stop-band ripple, stop-band attenuation is better assessed with the logarithmically scaled magnitude response (Fig. 1D and H) whereas pass-band ripple is better assessed with the linearly scaled magnitude response (Fig. 1C and G; see also Widmann et al., 2015). The shifted cut-off frequencies, resulting from the two-pass filtering, are demonstrated in the magnitude responses (Fig. 1C, D, G, and H).

The magnitude responses of the least-square FIR filters show excessive pass-band ripple (Fig. 1C and G), including non-unity DC gain for the low-pass filter (Fig. 1G; correspondingly, the step response never returns to one; Fig. 1F; see also Widmann et al., 2015; Widmann and Schröger, 2012). These effects are a result of poor filter design: the filter order of the least-square FIR filters was defined independently of the transition-band width; the designated filter order is too low to approximate a rectangular magnitude response (see also Widmann et al., 2015). The pass-band ripple of the windowed FIR filters is relatively small in amplitude and therefore not apparent in Fig. 1C and G. In turn, the Butterworth filters have flat magnitude responses, both in the pass band and stop band. The Hamming-windowed FIR filters have the steepest roll-off (Fig. 1C, D, G, and H) and longest impulse response (Fig. 1A and E), followed by least-square FIR, 3rd, 2nd, and 1st order Butterworth filters. Steeper roll-offs lead to larger sidelobes in the impulse response (Fig. 1A and E) and increased ringing artifacts in the step response (Fig. 1B and F; see also Rousselet, 2012; Widmann et al., 2015).

3.2. Grand-averaged ERP waveforms

The effect of different high-pass filters on the grand-averaged ERP waveforms elicited by S1 and S2 are shown in Figs. 2 and 3, respectively. The unfiltered condition (indicated by the black line) shows the grand-averaged waveforms with no high-pass filtering applied and serves as a reference for the filter-induced distortions. There was virtually no difference between the unfiltered and the 0.1-Hz high-pass filtered waveforms (Figs. 2 A and 3 A). Likewise, filtering with a 0.5-Hz cut-off only had a minor effect on the shape of the waveform (Figs. 2 B and 3 B). As the cut-off frequency was set at 1 Hz and above, considerable distortions of the waveform began to emerge: the higher the cut-off frequency, the more the ERP waveform was altered. With cut-offs of 1–5 Hz (Figs. 2 C–E and 3 C–E), the low-frequency information from the large-amplitude N100 component was shifted into the latency range of the mid-latency ERP components. As the spreading of a waveform introduced by high-pass filters is of opposite polarity, the spreading resulted in significantly increased amplitudes of the P50 compo-

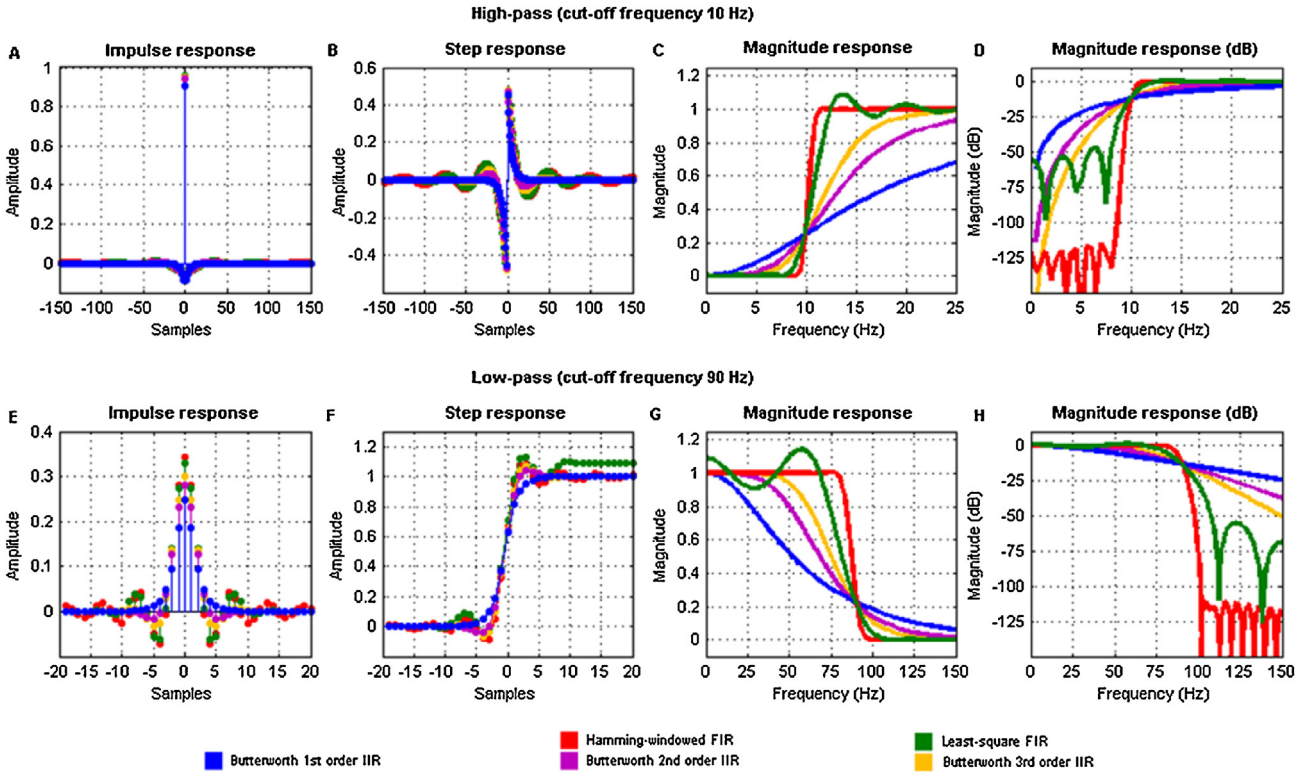

Fig. 1. An example of the filter responses of the designed zero-phase high-pass and low-pass filters. The impulse, step, and magnitude responses are shown for high-pass filters with a 10-Hz cut-off (panels A–D) and for low-pass filters with a 90-Hz cut-off (panels E–H). The shown responses apply to the final, two-pass filtering. The impulse and step responses describe a filter in the time domain, whereas the magnitude response (along with the phase response) describes a filter in the frequency domain. Filters with steeper roll-offs in their magnitude responses have longer impulse responses and increased ringing artifacts in the time domain.

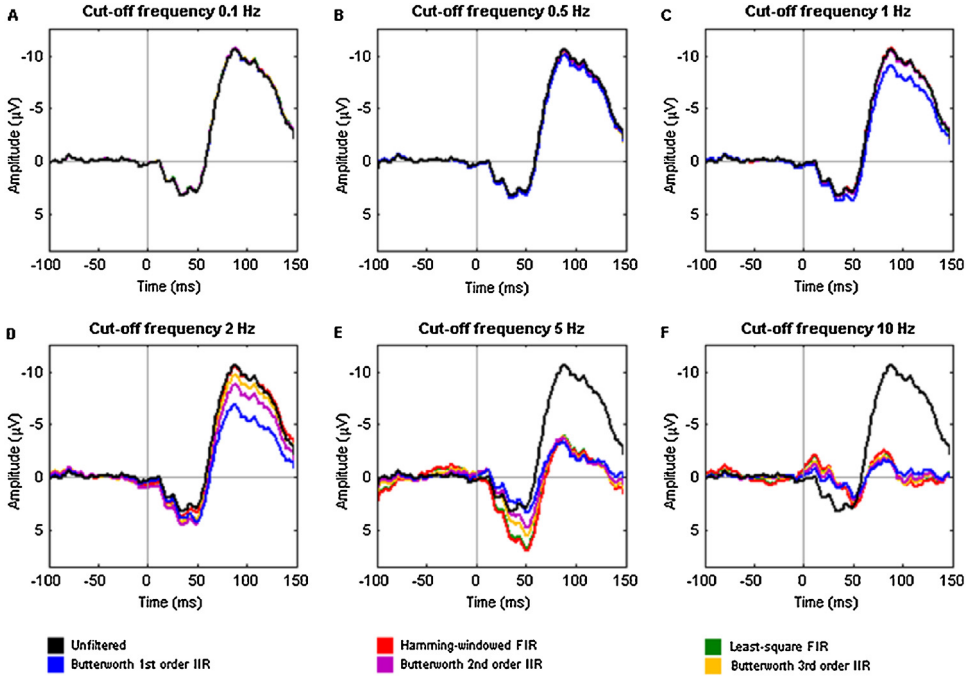

Fig. 2. The effect of different high-pass filters on the grand-averaged ERP waveforms at Cz electrode site elicited by the first stimulus sound (S1). The filtering of the EEG signals was repeated with a Hamming-windowed FIR, least-square FIR, and Butterworth (1st, 2nd, and 3rd order) IIR filters, prior to epoching or averaging. Each filter type was applied as a zero-phase high-pass filter having a cut-off at approximately 0.1 Hz (panel A), 0.5 Hz (panel B), 1 Hz (pane C), 2 Hz (panel D), 5 Hz (panel E), and 10 Hz (panel F; the cut-off frequencies refer to the half-amplitude (−6 dB) cut-off of the original, one-pass filter). The black line indicates grand-averaged waveforms with no high-pass filtering applied, serving as a reference for the filter-induced distortions. As the cut-off frequency of the high-pass filters was increased, the ERP waveform was distorted more severely.

Table 5
The effect of different high-pass filters on the P50 gating difference (S1–S2 difference), i.e., the P50 amplitude in response to the second stimulus sound (S2) subtracted from that of the first stimulus sound (S1). The Wilcoxon signed-rank test with two-tailed exact significance was used to determine whether there was a statistically significant difference in the median S1–S2 difference between the high-pass filtered and unfiltered waveforms. The median, first and third quartiles (Q1–Q3), and test statistics are reported for the S1–S2 difference as a function of filter type and high-pass cut-off frequency. In the unfiltered waveforms the S1–S2 difference was given a median of 1.90 μV (Q1–Q3 0.50–2.94 μV).

High-pass cut-off frequency	Filter type	S1–S2 difference				
		Median (μV)	Q1–Q3 (μV)	Test statistics[a]		
				Z-score	*p*-value	Effect size *r*
0.1 Hz	Hamming-windowed FIR	1.89	0.51–2.96	−0.68[c]	0.51	−0.090
	Least-square FIR	1.88	0.51–2.96	−0.65[c]	0.52	−0.087
	Butterworth 1st order IIR	1.84	0.51–2.95	−0.39[b]	0.71	−0.052
	Butterworth 2nd order IIR	1.89	0.50–2.95	−0.64[c]	0.54	−0.085
	Butterworth 3rd order IIR	1.89	0.51–2.96	−0.89[c]	0.38	−0.12
0.5 Hz	Hamming-windowed FIR	1.62	0.61–2.91	−0.068[b]	0.95	−0.009
	Least-square FIR	1.59	0.59–2.95	−0.31[c]	0.77	−0.041
	Butterworth 1st order IIR	1.56	0.59–2.73	−0.036[c]	0.98	−0.005
	Butterworth 2nd order IIR	1.60	0.55–2.90	−0.82[b]	0.42	−0.11
	Butterworth 3rd order IIR	1.61	0.57–2.92	−0.19[b]	0.85	−0.026
1 Hz	Hamming-windowed FIR	1.00	−0.20–2.79	−2.35[b]	**0.018**	−0.31*
	Least-square FIR	1.08	−0.08–2.88	−1.90[b]	0.058	−0.25
	Butterworth 1st order IIR	1.69	0.66–3.31	−1.18[c]	0.24	−0.16
	Butterworth 2nd order IIR	1.22	0.06–2.93	−1.36[b]	0.18	−0.18
	Butterworth 3rd order IIR	1.06	−0.09–2.85	−1.94[b]	0.053	−0.26
2 Hz	Hamming-windowed FIR	1.67	0.40–3.20	−0.82[c]	0.42	−0.11
	Least-square FIR	1.66	0.39–3.21	−0.79[c]	0.44	−0.11
	Butterworth 1st order IIR	1.79	0.98–3.53	−2.29[c]	**0.021**	−0.31*
	Butterworth 2nd order IIR	2.03	1.05–3.92	−2.78[c]	**0.004**	−0.37*
	Butterworth 3rd order IIR	2.05	0.93–3.74	−2.59[c]	**0.008**	−0.35*
5 Hz	Hamming-windowed FIR	3.23	1.73–4.90	−3.62[c]	**<0.001**	−0.48*
	Least-square FIR	2.63	1.27–4.48	−3.37[c]	**<0.001**	−0.45*
	Butterworth 1st order IIR	1.08	0.45–2.53	−0.54[b]	0.60	−0.071
	Butterworth 2nd order IIR	1.74	0.79–3.26	−1.66[c]	0.10	−0.22
	Butterworth 3rd order IIR	2.06	0.90–3.78	−2.38[c]	**0.016**	−0.32*
10 Hz	Hamming-windowed FIR	1.01	−0.25–2.05	−1.34[b]	0.18	−0.18
	Least-square FIR	1.02	−0.32–1.98	−1.50[b]	0.14	−0.20
	Butterworth 1st order IIR	0.51	0.12–1.51	−2.44[b]	**0.013**	−0.33*
	Butterworth 2nd order IIR	0.59	−0.09–1.74	−2.16[b]	**0.030**	−0.29
	Butterworth 3rd order IIR	0.68	−0.26–1.73	−1.91[b]	0.056	−0.26

Note: [a] Wilcoxon signed-rank test; [b] based on positive ranks; [c] based on negative ranks; statistical significance (***p* < 0.05**) indicated in **bold**.
* Medium effect ($0.3 \leq |r| < 0.5$).

nent. High-pass filtering with a 10-Hz cut-off did not increase the amplitude of the P50 component (Figs. 2 F and 3 F); in fact, the amplitudes of the mid-latency components were even decreased compared to the unfiltered waveform. Instead of increased amplitudes the 10-Hz cut-off introduced substantial oscillations into the waveform with a frequency near the cut-off frequency. This oscillating effect of filters may already be recognized with the 5-Hz cut-off (Figs. 2 E and 3 E).

The effect of different low-pass filters on the grand-averaged ERP waveforms elicited by S1 and S2 are shown in Figs. 4 and 5, respectively. Attenuating high-frequency noise with low-pass filters resulted in smoothened ERP waveforms, reduced peak amplitudes, and spreading of the onset and offset. The lower the cut-off frequency, the more severely the ERP waveform was altered. However, this was not the case for the least-square FIR filter for which the distortion of the waveform shape was even more severe with higher cut-offs; albeit the distortion caused by higher cut-offs was more significant on the N100 component than on the mid-latency components. Filtering with a cut-off at 60 Hz and below (Figs. 4 A–C and 5 A–C) led to earlier onsets and later offsets with each filter type, whereas with cut-offs at 70 Hz and above (Figs. 4 D–F and 5 D–F) the temporal spreading was mild, apart from the 1st order Butterworth filter. Accordingly, the reduction in the P50 amplitude was relatively modest with cut-offs at 70 Hz and above, apart from the 1st order Butterworth filter; the minimum attenuation was observed for the windowed FIR filter (as was already seen in the impulse responses in Fig. 1E). Filtering with the 1st order Butterworth filter resulted in maximum attenuation and notably reduced P50 amplitude at each cut-off frequency.

3.3. The statistical effects of high-pass filtering

Results from the Wilcoxon signed-rank test concerning the effects of high-pass filtering are presented in Tables 2–5. Compared to the unfiltered waveforms, the Wilcoxon signed-rank test indicated no statistically significant differences in the median S1 amplitude (Table 2), S2 amplitude (Table 3), S2/S1 ratio (Table 4), or S1–S2 difference (Table 5) when high-pass filters with a 0.1-Hz cut-off were applied.

With a 0.5-Hz cut-off, the median S1 was significantly increased for all filter types apart from the 2nd order Butterworth (Table 2); the median S2 was significantly increased for each filter (Table 3). The median S2/S1 ratio was significantly larger for the Butterworth filters (Table 4), whereas the S1–S2 differences indicated no significant effects (Table 5).

When filtered with a 1-Hz high-pass cut-off, the S1 amplitudes were significantly larger only for the 1st order Butterworth filter (Table 2) while the S2 amplitudes showed a significant increase for each filter (Table 3). The 1-Hz cut-off resulted in significantly larger S2/S1 ratios for the FIR and 2nd and 3rd order Butterworth filters (Table 4), but the S1–S2 differences showed a significant change

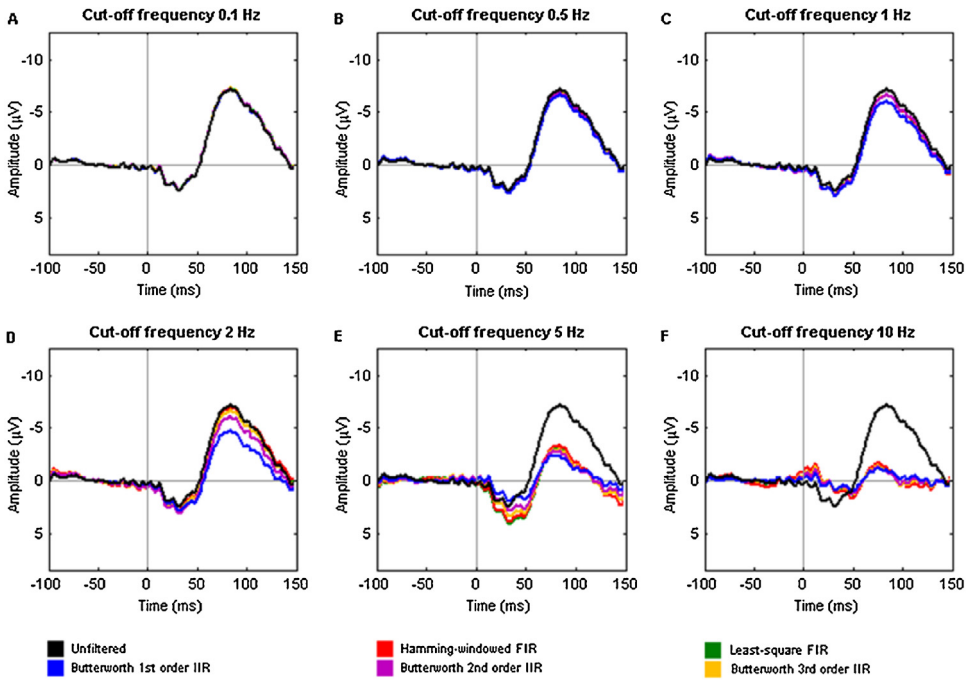

Fig. 3. The effect of different high-pass filters on the grand-averaged ERP waveforms at Cz electrode site elicited by the second stimulus sound (S2). The filtering of the EEG signals was repeated with a Hamming-windowed FIR, least-square FIR, and Butterworth (1st, 2nd, and 3rd order) IIR filters, prior to epoching or averaging. Each filter type was applied as a zero-phase high-pass filter having a cut-off at approximately 0.1 Hz (panel A), 0.5 Hz (panel B), 1 Hz (panel C), 2 Hz (panel D), 5 Hz (panel E), and 10 Hz (panel F; the cut-off frequencies refer to the half-amplitude (−6 dB) cut-off of the original, one-pass filter). The black line indicates grand-averaged waveforms with no high-pass filtering applied, serving as a reference for the filter-induced distortions. As the cut-off frequency of the high-pass filters was increased, the ERP waveform was distorted more severely.

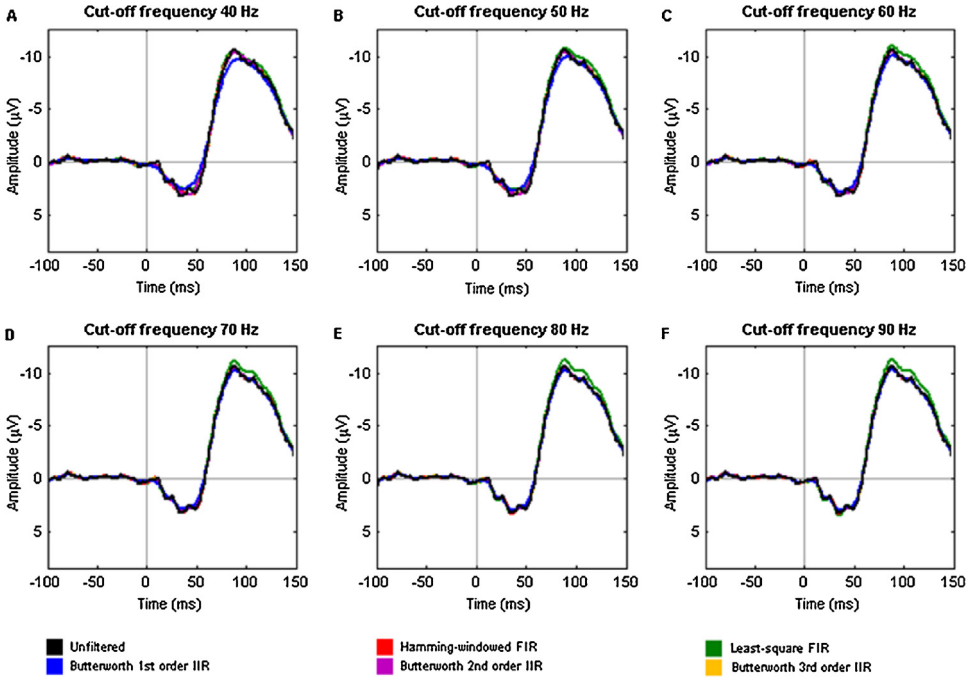

Fig. 4. The effect of different low-pass filters on the grand-averaged ERP waveforms at Cz electrode site elicited by the first stimulus sound (S1). The filtering of the EEG signals was repeated with a Hamming-windowed FIR, least-square FIR, and Butterworth (1st, 2nd, and 3rd order) IIR filters, prior to epoching or averaging. Each filter type was applied as a zero-phase low-pass filter having a cut-off at approximately 40 Hz (panel A), 50 Hz (panel B), 60 Hz (panel C), 70 Hz (panel D), 80 Hz (panel E), and 90 Hz (panel F; the cut-off frequencies refer to the half-amplitude (−6 dB) cut-off of the original, one-pass filter). The black line indicates grand-averaged waveforms with no low-pass filtering applied, serving as a reference for the filter-induced distortions. Attenuating high-frequency noise with low-pass filters resulted in smoothened ERP waveforms, reduced peak amplitudes, and spreading of the onset and offset. The lower the cut-off frequency, the more the peak amplitudes were reduced.

only for the windowed FIR filter with reduced S1–S2 differences (Table 5).

A high-pass cut-off at 2 Hz produced significantly larger S1 amplitudes for each Butterworth filter (Table 2) while the S2 amplitudes were significantly larger for each filter type (Table 3). The

Table 6
The effect of different low-pass filters on the P50 amplitude (S1 amplitude) in response to the first stimulus sound (S1). The Wilcoxon signed-rank test with two-tailed exact significance was used to determine whether there was a statistically significant difference in the median S1 amplitude between the low-pass filtered and unfiltered waveforms. The median, first and third quartiles (Q1–Q3), and test statistics are reported for the S1 amplitude as a function of filter type and low-pass cut-off frequency. In the unfiltered waveforms the S1 amplitude was given a median of 4.63 μV (Q1–Q3 3.43–6.22 μV).

Low-pass cut-off frequency	Filter type	S1 amplitude				
		Median (μV)	Q1–Q3 (μV)	Test statistics[a]		
				Z-score	*p*-value	Effect size *r*
40 Hz	Hamming-windowed FIR	3.57	2.37–5.32	−4.60[b]	**<0.001**	−0.61**
	Least-square FIR	3.11	2.06–4.97	−4.62[b]	**<0.001**	−0.62**
	Butterworth 1st order IIR	2.45	1.26–4.03	−4.62[b]	**<0.001**	−0.62**
	Butterworth 2nd order IIR	3.10	2.15–5.14	−4.60[b]	**<0.001**	−0.61**
	Butterworth 3rd order IIR	3.25	2.31–5.32	−4.60[b]	**<0.001**	−0.61**
50 Hz	Hamming-windowed FIR	3.67	2.69–5.54	−4.49[b]	**<0.001**	−0.60**
	Least-square FIR	3.35	2.23–5.18	−4.62[b]	**<0.001**	−0.62**
	Butterworth 1st order IIR	2.77	1.60–4.45	−4.62[b]	**<0.001**	−0.62**
	Butterworth 2nd order IIR	3.42	2.34–5.27	−4.60[b]	**<0.001**	−0.61**
	Butterworth 3rd order IIR	3.58	2.50–5.34	−4.60[b]	**<0.001**	−0.61**
60 Hz	Hamming-windowed FIR	3.78	2.74–5.59	−4.40[b]	**<0.001**	−0.59**
	Least-square FIR	3.55	2.39–5.45	−4.48[b]	**<0.001**	−0.60**
	Butterworth 1st order IIR	3.03	1.85–4.78	−4.62[b]	**<0.001**	−0.62**
	Butterworth 2nd order IIR	3.56	2.54–5.32	−4.62[b]	**<0.001**	−0.62**
	Butterworth 3rd order IIR	3.62	2.68–5.42	−4.62[b]	**<0.001**	−0.62**
70 Hz	Hamming-windowed FIR	3.73	3.02–5.80	−4.13[b]	**<0.001**	−0.55**
	Least-square FIR	3.71	2.62–5.65	−4.31[b]	**<0.001**	−0.58**
	Butterworth 1st order IIR	3.20	2.06–4.94	−4.62[b]	**<0.001**	−0.62**
	Butterworth 2nd order IIR	3.60	2.69–5.41	−4.62[b]	**<0.001**	−0.62**
	Butterworth 3rd order IIR	3.66	2.76–5.51	−4.62[b]	**<0.001**	−0.62**
80 Hz	Hamming-windowed FIR	3.69	3.21–5.68	−3.53[b]	**<0.001**	−0.47*
	Least-square FIR	3.74	2.81–5.79	−3.96[b]	**<0.001**	−0.53**
	Butterworth 1st order IIR	3.31	2.25–5.06	−4.62[b]	**<0.001**	−0.62**
	Butterworth 2nd order IIR	3.64	2.79–5.49	−4.62[b]	**<0.001**	−0.62**
	Butterworth 3rd order IIR	3.68	2.91–5.57	−4.54[b]	**<0.001**	−0.61**
90 Hz	Hamming-windowed FIR	3.69	3.18–5.83	−3.55[b]	**<0.001**	−0.47*
	Least-square FIR	3.72	3.01–5.89	−3.60[b]	**<0.001**	−0.48*
	Butterworth 1st order IIR	3.38	2.42–5.15	−4.62[b]	**<0.001**	−0.62**
	Butterworth 2nd order IIR	3.65	2.90–5.54	−4.62[b]	**<0.001**	−0.62**
	Butterworth 3rd order IIR	3.68	3.10–5.68	−4.47[b]	**<0.001**	−0.60**

Note: [a] Wilcoxon signed-rank test; [b] based on positive ranks; statistical significance (***p* < 0.05**) indicated in **bold**.
* Medium effect ($0.3 \leq |r| < 0.5$).
** Large effect ($|r| \geq 0.5$).

2-Hz cut-off did not introduce significant changes in the median S2/S1 ratio (Table 4), but the median S1–S2 difference was again larger for each Butterworth filter (Table 5).

Filtering with a 5-Hz cut-off resulted in a significant increase in the median S1 (Table 2) and S2 amplitude (Table 3), except for the 1st order Butterworth filter. However, the 5-Hz cut-off introduced no significant median changes in the S2/S1 ratio (Table 4). The S1–S2 differences were significantly increased for the FIR and 3rd order Butterworth filters (Table 5).

The median S1-amplitude was significantly smaller when high-pass filtered with a 10-Hz cut-off for each filter type (Table 2) whereas the median S2-amplitude was significantly smaller only when Butterworth filters were applied (Table 3). The 10-Hz cut-off revealed no significant changes in the S2/S1 ratios (Table 4), and the S1–S2 differences were significantly reduced only for the 1st and 2nd order Butterworth filters (Table 5).

3.4. The statistical effects of low-pass filtering

Results from the Wilcoxon signed-rank test concerning the effects of low-pass filtering are presented in Tables 6–9. Compared to the unfiltered waveforms, the Wilcoxon signed-rank test indicated a statistically significant decrease in the median S1 amplitude (Table 6) and S2 amplitude (Table 7) for each filter type and cut-off frequency. However, the significant differences in the median S2/S1 ratio and S1–S2 difference were fewer. The median S2/S1 ratio (Table 8) was significantly decreased when a Hamming-windowed FIR filter with a 60-Hz cut-off was applied. In addition, the S2/S1 ratios were significantly smaller for the 3rd order Butterworth filter with cut-offs at 70, 80, and 90 Hz, as well as the 2nd order Butterworth filter with cut-offs at 80 and 90 Hz. Filtering with the 1st order Butterworth filter resulted in significantly reduced S1–S2 differences (Table 9) at each cut-off frequency. Significantly smaller S1–S2 differences were also observed for the least-square FIR and 2nd order Butterworth filters with a 40-Hz cutoff.

3.5. Filtering a simulated ERP waveform

As the changes in the scalp-recorded voltage that give rise to the ERP waveform reflect the summation of spatially and temporally overlapping postsynaptic potentials, the true waveform for a single component is not known in real recordings. Therefore, the experimental data were supplemented with a simulated waveform comprising the artificial components P50, N100, and P200 (Fig. 6). The simulated ERP waveform was generated from the sum of three Gaussians (embedded in zero values to avoid edge artifacts): $f(t|\mu,\sigma) = \Sigma_{i=1}^{3} A_i e^{-(t-\mu_i)^2/2\sigma_i^2}$, where $A_1 = 3$ μV, $\mu_1 = 0.05$ s, $\sigma_1 = 0.01$ s; $A_2 = -10$ μV, $\mu_2 = 0.1$ s, $\sigma_2 = 0.025$ s; $A_3 = 5$ μV, $\mu_3 = 0.2$ s, $\sigma_3 = 0.03$ s. The simulated ERP waveform was high-pass filtered with zero-phase Hamming-windowed sinc FIR filters having cut-offs at approximately 0.1 Hz, 0.5 Hz, 1 Hz, 2 Hz, 5 Hz, and 10 Hz.

Table 7
The effect of different low-pass filters on the P50 amplitude (S2 amplitude) in response to the second stimulus sound (S2). The Wilcoxon signed-rank test with two-tailed exact significance was used to determine whether there was a statistically significant difference in the median S2 amplitude between the low-pass filtered and unfiltered waveforms. The median, first and third quartiles (Q1–Q3), and test statistics are reported for the S2 amplitude as a function of filter type and low-pass cut-off frequency. In the unfiltered waveforms the S2 amplitude was given a median of 3.46 μV (Q1–Q3 2.52–4.46 μV).

Low-pass cut-off frequency	Filter type	S2 amplitude				
		Median (μV)	Q1–Q3 (μV)	Test statistics[a]		
				Z-score	*p*-value	Effect size *r*
40 Hz	Hamming-windowed FIR	2.63	1.54–3.73	−4.62[b]	**<0.001**	−0.62**
	Least-square FIR	2.22	1.32–3.47	−4.62[b]	**<0.001**	−0.62**
	Butterworth 1st order IIR	1.67	0.83–2.62	−4.62[b]	**<0.001**	−0.62**
	Butterworth 2nd order IIR	2.26	1.36–3.39	−4.62[b]	**<0.001**	−0.62**
	Butterworth 3rd order IIR	2.32	1.45–3.58	−4.62[b]	**<0.001**	−0.62**
50 Hz	Hamming-windowed FIR	2.67	1.88–4.01	−4.62[b]	**<0.001**	−0.62**
	Least-square FIR	2.48	1.58–3.72	−4.62[b]	**<0.001**	−0.62**
	Butterworth 1st order IIR	1.84	1.12–2.96	−4.62[b]	**<0.001**	−0.62**
	Butterworth 2nd order IIR	2.34	1.57–3.63	−4.62[b]	**<0.001**	−0.62**
	Butterworth 3rd order IIR	2.48	1.68–3.78	−4.62[b]	**<0.001**	−0.62**
60 Hz	Hamming-windowed FIR	2.73	1.97–4.42	−4.30[b]	**<0.001**	−0.58**
	Least-square FIR	2.53	1.85–4.17	−4.60[b]	**<0.001**	−0.61**
	Butterworth 1st order IIR	2.02	1.32–3.20	−4.62[b]	**<0.001**	−0.62**
	Butterworth 2nd order IIR	2.45	1.72–3.81	−4.62[b]	**<0.001**	−0.62**
	Butterworth 3rd order IIR	2.47	1.79–4.00	−4.62[b]	**<0.001**	−0.62**
70 Hz	Hamming-windowed FIR	2.69	2.00–4.37	−4.16[b]	**<0.001**	−0.56**
	Least-square FIR	2.67	2.01–4.37	−4.44[b]	**<0.001**	−0.59**
	Butterworth 1st order IIR	2.16	1.50–3.38	−4.62[b]	**<0.001**	−0.62**
	Butterworth 2nd order IIR	2.53	1.81–3.98	−4.62[b]	**<0.001**	−0.62**
	Butterworth 3rd order IIR	2.48	1.89–4.18	−4.62[b]	**<0.001**	−0.62**
80 Hz	Hamming-windowed FIR	2.87	1.93–4.37	−4.33[b]	**<0.001**	−0.58**
	Least-square FIR	2.74	2.04–4.40	−4.36[b]	**<0.001**	−0.58**
	Butterworth 1st order IIR	2.28	1.63–3.52	−4.62[b]	**<0.001**	−0.62**
	Butterworth 2nd order IIR	2.62	1.91–4.09	−4.62[b]	**<0.001**	−0.62**
	Butterworth 3rd order IIR	2.73	1.99–4.26	−4.60[b]	**<0.001**	−0.61**
90 Hz	Hamming-windowed FIR	3.04	2.13–4.33	−4.12[b]	**<0.001**	−0.55**
	Least-square FIR	2.94	2.03–4.39	−4.33[b]	**<0.001**	−0.58**
	Butterworth 1st order IIR	2.37	1.72–3.63	−4.62[b]	**<0.001**	−0.62**
	Butterworth 2nd order IIR	2.73	1.98–4.16	−4.62[b]	**<0.001**	−0.62**
	Butterworth 3rd order IIR	2.81	2.05–4.28	−4.56[b]	**<0.001**	−0.61**

Note: [a] Wilcoxon signed-rank test; [b] based on positive ranks; statistical significance (***p* < 0.05**) indicated in **bold**.
** Large effect ($|r| \geq 0.5$).

The distortions in the simulated ERP waveform introduced by high-pass filtering were similar as in the grand-averaged ERP waveforms. There was virtually no difference between the unfiltered and the 0.1-Hz high-pass filtered waveform, and the waveform distortion was mild when filtered with a 0.5-Hz cut-off. As the cut-off frequency was set at 1–5 Hz, the low-frequency information from the large-amplitude N100 component was shifted into the latency range of the P50 component with positive polarity: the higher the cut-off frequency, the more the P50 amplitude was increased. High-pass filtering with a 10-Hz cut-off did not augment the P50 amplitude but instead introduced substantial oscillations; oscillations were also present with the 5-Hz cut-off.

4. Discussion

The present study confirms that filtering has a significant impact on the amplitude and gating measures of the P50 component; application of improper filter parameters results in substantial distortions of the ERP waveform, possibly leading to completely false conclusions. Differences in the used filter settings, along with other methodological differences, make it difficult to compare results across studies and to evaluate the true existence of auditory sensory gating deficit in Alzheimer's disease.

The majority of studies on sensory gating report using a high-pass filter with a 10-Hz cut-off to measure P50 suppression. Literature does not, however, provide justified arguments in favor of applying such a relatively high cut-off, other than the objective of removing the influence of the N100 and P200 components. Indeed, according to the results of the present study, increasing the high-pass cut-off frequency markedly augments the P50 component. The grand-averaged ERP waveforms demonstrated how setting the cut-off frequency at 0.5 Hz and above began to increase the P50 amplitude, in response to both S1 (Fig. 2) and S2 (Fig. 3). However, this seemed to be a consequence of a filter-induced distortion shifting the low-frequency information from the large-amplitude, later components into the latency range of the P50. Increasing the cut-off frequency to 10 Hz no longer increased the P50 amplitude but instead introduced artificial oscillations. In fact, the 10-Hz cut-off resulted in statistically significant decrease in the S1 amplitude for each filter type (Table 2), although the S2 amplitude was significantly decreased only for Butterworth filters (Table 3). The oscillating effect of the filters was already visible when filtered with a 5-Hz cut-off (Fig. 2 and Fig. 3). The distortions in the simulated ERP waveform introduced by high-pass filtering (Fig. 6) were consistent with the distortions in the grand-averaged ERP waveforms.

Despite the numerous significant changes in the S1 (Table 2) and S2 amplitudes (Table 3), only a few high-pass filter settings resulted in significantly changed S2/S1 ratios (Table 4) or S1–S2 differences (Table 5). Therefore, it may be concluded that the change in both the S1 and S2 amplitude was of similar magnitude for most high-pass filters and thereby cancelled out in the S2/S1 ratio and S1–S2 difference (see also Freedman et al., 1998). However, recent literature

Table 8
The effect of different low-pass filters on the P50 gating ratio (S2/S1 ratio), i.e., the ratio of the P50 amplitude in response to the second stimulus sound (S2) relative to that of the first stimulus sound (S1). The Wilcoxon signed-rank test with two-tailed exact significance was used to determine whether there was a statistically significant difference in the median S2/S1 ratio between the low-pass filtered and unfiltered waveforms. The median, first and third quartiles (Q1–Q3), and test statistics are reported for the S2/S1 ratio as a function of filter type and low-pass cut-off frequency. In the unfiltered waveforms the S2/S1 ratio was given a median of 0.66 (Q1–Q3 0.43–0.89).

Low-pass cut-off frequency	Filter type	S2/S1 ratio				
		Median	Q1–Q3	Test statistics[a]		
				Z-score	*p*-value	Effect size *r*
40 Hz	Hamming-windowed FIR	0.63	0.39–0.99	−1.89[b]	0.060	−0.25
	Least-square FIR	0.59	0.28–1.00	−1.41[b]	0.16	−0.19
	Butterworth 1st order IIR	0.68	0.28–1.02	−1.53[b]	0.13	−0.20
	Butterworth 2nd order IIR	0.63	0.39–1.04	−1.09[b]	0.28	−0.15
	Butterworth 3rd order IIR	0.62	0.37–0.99	−1.82[b]	0.070	−0.24
50 Hz	Hamming-windowed FIR	0.66	0.39–0.96	−1.66[b]	0.10	−0.22
	Least-square FIR	0.67	0.34–0.95	−1.71[b]	0.090	−0.23
	Butterworth 1st order IIR	0.67	0.36–1.01	−1.23[b]	0.23	−0.16
	Butterworth 2nd order IIR	0.62	0.37–0.97	−1.73[b]	0.086	−0.23
	Butterworth 3rd order IIR	0.62	0.37–0.99	−1.78[b]	0.077	−0.24
60 Hz	Hamming-windowed FIR	0.65	0.38–0.98	−2.00[b]	**0.045**	−0.27
	Least-square FIR	0.66	0.34–0.96	−1.44[b]	0.16	−0.19
	Butterworth 1st order IIR	0.67	0.36–1.01	−1.09[b]	0.28	−0.15
	Butterworth 2nd order IIR	0.63	0.36–0.97	−1.75[b]	0.081	−0.23
	Butterworth 3rd order IIR	0.64	0.37–0.98	−1.96[b]	0.050	−0.26
70 Hz	Hamming-windowed FIR	0.66	0.40–0.94	−1.73[b]	0.086	−0.23
	Least-square FIR	0.69	0.36–0.95	−1.94[b]	0.053	−0.26
	Butterworth 1st order IIR	0.69	0.35–1.01	−1.03[b]	0.32	−0.14
	Butterworth 2nd order IIR	0.64	0.37–0.96	−1.80[b]	0.074	−0.24
	Butterworth 3rd order IIR	0.66	0.38–0.96	−2.00[b]	**0.045**	−0.27
80 Hz	Hamming-windowed FIR	0.65	0.42–0.92	−1.80[b]	0.074	−0.24
	Least-square FIR	0.68	0.40–0.92	−1.94[b]	0.053	−0.26
	Butterworth 1st order IIR	0.66	0.34–0.95	−1.66[b]	0.10	−0.22
	Butterworth 2nd order IIR	0.66	0.38–0.95	−2.03[b]	**0.043**	−0.27
	Butterworth 3rd order IIR	0.66	0.39–0.94	−2.14[b]	**0.032**	−0.29
90 Hz	Hamming-windowed FIR	0.67	0.41–0.91	−1.21[b]	0.24	−0.16
	Least-square FIR	0.66	0.42–0.91	−1.89[b]	0.060	−0.25
	Butterworth 1st order IIR	0.66	0.34–0.95	−1.78[b]	0.077	−0.24
	Butterworth 2nd order IIR	0.66	0.39–0.93	−2.35[b]	**0.018**	−0.31*
	Butterworth 3rd order IIR	0.66	0.40–0.92	−2.30[b]	**0.020**	−0.31*

Note: [a] Wilcoxon signed-rank test; [b] based on positive ranks; statistical significance ($p < 0.05$) indicated in **bold**.
* Medium effect ($0.3 \leq |r| < 0.5$).

has proposed that rather than the S2/S1 ratio or S1–S2 difference, the S1 and S2 amplitudes should be assessed in terms of sensory gating (Toyomaki et al., 2015).

The only high-pass cut-off frequency that did not introduce significant changes in any of the variables, i.e., the S1 amplitude (Table 2), S2 amplitude (Table 3), S2/S1 ratio (Table 4), or S1–S2 difference (Table 5), was 0.1 Hz, regardless of the filter type. Based on these findings, high-pass filters with cut-offs at 0.1 Hz may be recommended for the optimal balance between noise reduction and distortion of the P50 component. The authors advise against using the traditional 10-Hz cut-off due to the substantial distortions it appears to introduce. As clearly demonstrated in Fig. 6, high-pass filtering with a 10-Hz cut-off resulted in prominent artificial oscillations in the simulated ERP waveform: the high-pass filtered waveform may even be thought to closely resemble a pure sinusoid with a frequency near the cut-off frequency. These kinds of artificial oscillations could create the appearance of spurious oscillatory activity in an experimental effect that was not present in the original waveform (see also Luck, 2014; Yeung et al., 2007).

Auditory sensory gating is a multistage operation indexed by the suppression of the P50, N100, and P200 responses to repeated auditory stimuli (Boutros et al., 2004). The P50, N100, and P200 components are considered to reflect different phases of information processing: pre-attentive (P50), early attentive (N100), and later attentive (P200). As setting the high-pass filter cut-off at 0.5 Hz and above resulted in markedly decreased N100 amplitudes accompanied with a substantial but artificial increase in the P50 amplitudes, inappropriate high-pass filters might lead researchers to draw bogus conclusions on which cognitive processes were engaged within a given experimental manipulation: excessive high-pass filtering makes it presumptuous to conclude whether the given experimental manipulation affected the P50, N100, or both. It should also be accounted for that the artificial effects introduced by severe high-pass filtering may manifest themselves unequally on different subject groups. Slowing down of the EEG rhythms is characteristic of Alzheimer's disease: the power in the lower frequencies, i.e., delta (< 4 Hz) and theta (4–8 Hz), is increased, and the power in the higher frequencies, i.e., alpha (8–13 Hz) and beta (13–30 Hz), is decreased (Jeong, 2004). As the present study proposes that the augmentation of the P50 component introduced by high-pass filtering is a consequence of a filter-induced distortion shifting the low-frequency information from the N100 component into the latency range of the P50, the distortion of the P50 might be less severe (or at least different) in healthy elderly subjects with less power in the lower frequencies, particularly in the theta band; theta has been suggested to mostly contribute to the N100 response (Brockhaus-Dumke et al., 2008). These differences in the frequency content might lead to incorrect results when comparing the amplitude and gating measures of the P50 between healthy elderly and patients with Alzheimer's disease.

The low-pass filtered grand-averaged waveforms demonstrated how attenuating high-frequency noise results in smoothened ERP waveforms, reduced peak amplitudes, and spreading of the onset and offset times (Figs. 4 and 5). Apart from the 1st order Butter-

Table 9
The effect of different low-pass filters on the P50 gating difference (S1–S2 difference), i.e., the P50 amplitude in response to the second stimulus sound (S2) subtracted from that of the first stimulus sound (S1). The Wilcoxon signed-rank test with two-tailed exact significance was used to determine whether there was a statistically significant difference in the median S1–S2 difference between the low-pass filtered and unfiltered waveforms. The median, first and third quartiles (Q1–Q3), and test statistics are reported for the S1–S2 difference as a function of filter type and low-pass cut-off frequency. In the unfiltered waveforms the S1–S2 difference was given a median of 1.90 μV (Q1–Q3 0.50–2.94 μV).

Low-pass cut-off frequency	Filter type	S1–S2 difference				
		Median (μV)	Q1–Q3 (μV)	Test statistics[a]		
				Z-score	*p*-value	Effect size *r*
40 Hz	Hamming-windowed FIR	1.36	0.02–2.41	−1.72[b]	0.087	−0.23
	Least-square FIR	1.20	0.01–2.34	−2.59[b]	**0.008**	−0.35*
	Butterworth 1st order IIR	0.78	0.02–1.85	−2.93[b]	**0.002**	−0.39*
	Butterworth 2nd order IIR	1.08	0.12–2.45	−2.02[b]	**0.043**	−0.27
	Butterworth 3rd order IIR	1.13	0.04–2.55	−1.92[b]	0.054	−0.26
50 Hz	Hamming-windowed FIR	1.27	0.13–2.59	−0.50[b]	0.63	−0.067
	Least-square FIR	1.15	0.18–2.44	−1.36[b]	0.18	−0.18
	Butterworth 1st order IIR	0.83	0.07–1.93	−2.81[b]	**0.004**	−0.38*
	Butterworth 2nd order IIR	1.06	0.09–2.58	−1.75[b]	0.080	−0.23
	Butterworth 3rd order IIR	1.10	0.05–2.61	−1.64[b]	0.10	−0.22
60 Hz	Hamming-windowed FIR	1.29	0.05–2.68	−0.36[b]	0.72	−0.049
	Least-square FIR	1.23	0.11–2.52	−0.52[b]	0.61	−0.070
	Butterworth 1st order IIR	0.86	0.11–1.99	−2.63[b]	**0.007**	−0.35*
	Butterworth 2nd order IIR	1.05	0.10–2.57	−1.51[b]	0.13	−0.20
	Butterworth 3rd order IIR	1.17	0.08–2.62	−0.91[b]	0.37	−0.12
70 Hz	Hamming-windowed FIR	1.59	0.25–2.98	−0.15[b]	0.89	−0.020
	Least-square FIR	1.40	0.17–2.76	−0.15[b]	0.89	−0.020
	Butterworth 1st order IIR	0.92	0.14–2.10	−2.51[b]	**0.011**	−0.33*
	Butterworth 2nd order IIR	1.12	0.16–2.63	−1.06[b]	0.30	−0.14
	Butterworth 3rd order IIR	1.28	0.16–2.74	−0.42[b]	0.68	−0.056
80 Hz	Hamming-windowed FIR	1.58	0.36–2.86	−0.32[c]	0.76	−0.043
	Least-square FIR	1.34	0.36–2.98	−0.34[c]	0.75	−0.045
	Butterworth 1st order IIR	0.97	0.17–2.19	−2.61[b]	**0.008**	−0.35*
	Butterworth 2nd order IIR	1.31	0.23–2.69	−0.88[b]	0.39	−0.12
	Butterworth 3rd order IIR	1.50	0.24–2.84	−0.19[b]	0.85	−0.026
90 Hz	Hamming-windowed FIR	1.46	0.38–2.90	−0.25[c]	0.81	−0.034
	Least-square FIR	1.43	0.40–3.03	−0.38[c]	0.72	−0.050
	Butterworth 1st order IIR	1.04	0.19–2.45	−2.33[b]	**0.018**	−0.31*
	Butterworth 2nd order IIR	1.48	0.28–2.75	−0.51[b]	0.62	−0.068
	Butterworth 3rd order IIR	1.67	0.33–2.93	−0.060[b]	0.96	−0.008

Note: [a] Wilcoxon signed-rank test; [b] based on positive ranks; [c]based on negative ranks; statistical significance ($p < 0.05$) indicated in **bold**.
* Medium effect ($0.3 \leq |r| < 0.5$).

worth filter, filtering with cut-offs at 70 Hz and above yielded only mild temporal smearing of the grand-averaged waveforms, accompanied with a modest P50 amplitude decrease. However, statistical tests indicated a significant decrease in the S1 (Table 6) and S2 amplitudes (Table 7) for each cut-off frequency and filter type. Again, the effect appeared to be of similar magnitude for both the S1 and S2 amplitude as statistically significant decreases in the median S2/S1 ratio (Table 8) and S1–S2 difference (Table 9) were fewer.

When evaluating the practical importance of the statistical significances in the S1 and S2 amplitudes, the purpose of low-pass filtering needs to be taken into account: low-pass filters are applied to eliminate high-frequency noise in the acquired EEG signals, thus resulting in altered ERP waveforms. If the filter did not introduce any changes into the signal, there would be no need for the filter (see also Widmann et al., 2015). When the P50 component is to be investigated, it is crucial to find the optimal low-pass cut-off frequency: the cut-off frequency should not be set too low in order for the high-frequency gamma activity to pass the filter; on the other hand, a cut-off frequency higher than necessary makes it harder to accurately interpret the waveforms. Results of this study suggest that a low-pass cut-off at 90 Hz or even above would be an optimal choice for analyses of the P50 component.

A least-square FIR filter has been the default FIR filter in EEGLAB toolbox (Delorme and Makeig, 2004) until the EEGLAB version 11.0.1.0b, and thus widely used in earlier ERP studies. It has, however, been stated since that using least-square FIR filters in ERP analyses is no longer recommended (see Widmann and Schröger, 2012; Widmann et al., 2015). As the present study pursued to provide evidence on the validity of previous sensory gating studies, least-square FIR filters were included in the analyses. Indeed, the present study confirmed the excessive ringing artifacts, substantial pass-band ripple, as well as non-unity DC gain introduced by least-square FIR filters (Fig. 1). However, the high-pass least-square FIR filters did not introduce any more statistically significant changes (Tables 2–5) or distortions of the waveform shape (Figs. 2 and 3) than what was introduced by windowed FIR filters; this applied also to the amount of statistically significant changes introduced by low-pass FIR filters (Tables 6–9). However, low-pass filtering with least-square FIR filters resulted in substantial distortions of the grand-averaged waveform (Figs. 4 and 5), although the distortions were more prominent on the N100 component than on the mid-latency components. Based on these results, the authors agree on avoiding the application of least-square FIR filters in ERP studies.

The authors would recommend using windowed sinc FIR filters in the analyses of the P50 component. With the windowing method, the stop-band attenuation and pass-band ripple of the filter can be precisely controlled by selection of a suitable window type (see, e.g., Mitra, 2011). In addition, the order of the windowed sinc FIR filter can be estimated to meet the desired transition-band width. However, if the recommended high-pass cut-off frequency of 0.1 Hz is applied, there are no arguments against using a high-pass Butterworth filter instead: neither the 1st, 2nd, nor 3rd order Butterworth

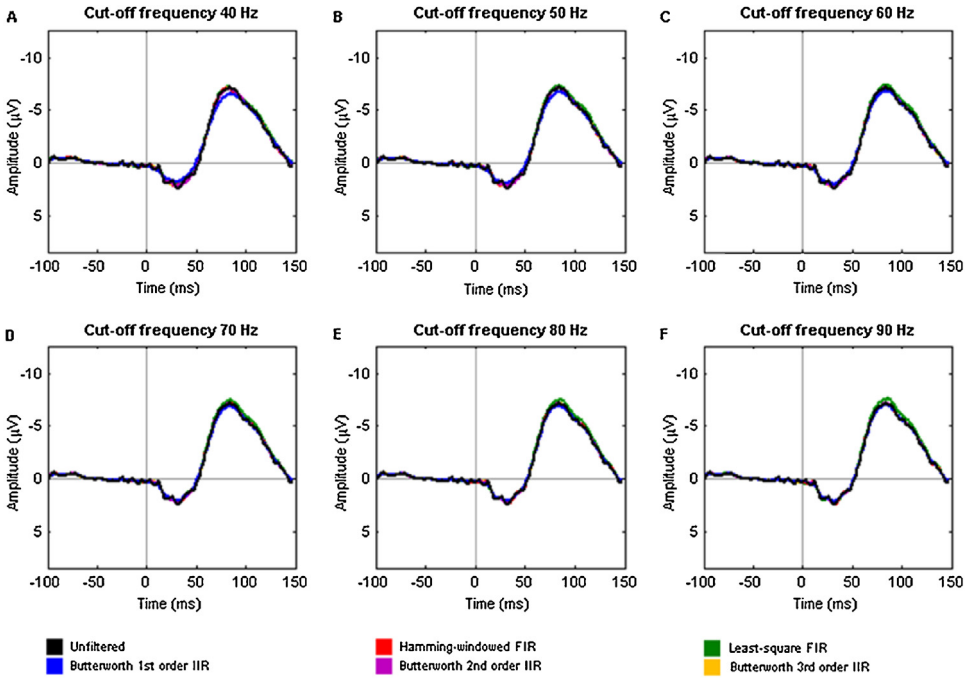

Fig. 5. The effect of different low-pass filters on the grand-averaged ERP waveforms at Cz electrode site elicited by the second stimulus sound (S2). The filtering of the EEG signals was repeated with a Hamming-windowed FIR, least-square FIR, and Butterworth (1st, 2nd, and 3rd order) IIR filters, prior to epoching or averaging. Each filter type was applied as a zero-phase low-pass filter having a cut-off at approximately 40 Hz (panel A), 50 Hz (panel B), 60 Hz (panel C), 70 Hz (panel D), 80 Hz (panel E), and 90 Hz (panel F; the cut-off frequencies refer to the half-amplitude (−6 dB) cut-off of the original, one-pass filter). The black line indicates grand-averaged waveforms with no low-pass filtering applied, serving as a reference for the filter-induced distortions. Attenuating high-frequency noise with low-pass filters resulted in smoothened ERP waveforms, reduced peak amplitudes, and spreading of the onset and offset. The lower the cut-off frequency, the more the peak amplitudes were reduced.

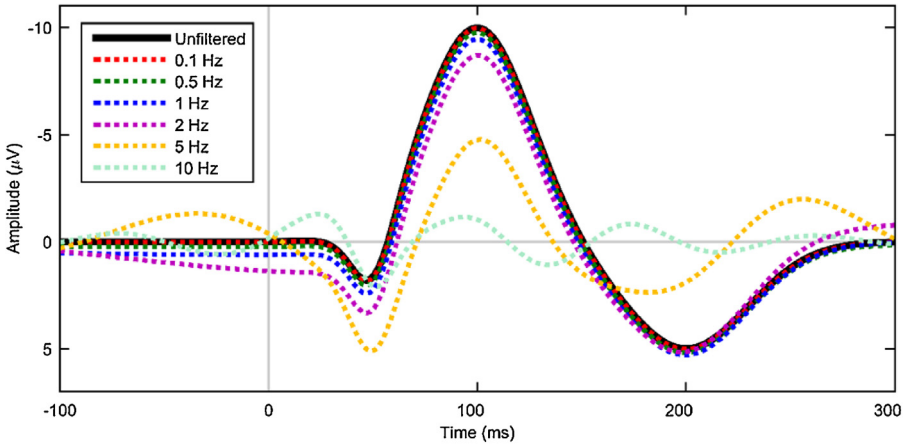

Fig. 6. High-pass filtering a simulated ERP waveform. The simulated ERP waveform comprising the artificial components P50, N100, and P200 was high-pass filtered with zero-phase Hamming-windowed FIR filters having cut-offs at approximately 0.1 Hz, 0.5 Hz, 1 Hz, 2 Hz, 5 Hz, and 10 Hz (the cut-off frequencies refer to the half-amplitude (−6 dB) cut-off of the original, one-pass filter). The black line indicates the simulated ERP waveform with no high-pass filtering applied, serving as a reference for the filter-induced distortions. As the cut-off frequency of the Hamming-windowed high-pass FIR filter was increased, the artificial ERP waveform was distorted more severely.

filter introduced significant changes in the S1 amplitude (Table 2), S2 amplitude (Table 3), S2/S1 ratio (Table 4), or S1–S2 difference (Table 5) when the 0.1 Hz high-pass cut-off was used. However, if a low-pass Butterworth filter is to be applied, the authors recommend using a higher cut-off frequency and/or steeper roll-off than what were used in the present study. As could already be predicted from the magnitude responses of the low-pass filters with a cut-off at 90 Hz (Fig. 1G), the attenuation of the 1st order Butterworth filter was excessive in the frequency range presumably contributing to the P50 component. Similarly, the 2nd and 3rd order Butterworth filters appeared to have notable attenuation in the frequency ranges of interest in P50 studies. Indeed, low-pass filtering with a 90-Hz 1st order Butterworth filter resulted in notably reduced P50 amplitude of the grand-averaged waveform (Figs. 4 F and 5 F) as well as a statistically decreased median S1–S2 difference (Table 9), although the S2/S1 ratio (Table 8) did not indicate a significant change. On the contrary, the low-pass 2nd and 3rd order Butterworth filters produced a statistically significant decrease in the S2/S1 ratio (Table 8) but not in the S1–S2 difference (Table 9) when the 90-Hz cut-off was used.

The variation of sensory gating results across studies clearly cannot originate solely from divergent filter settings; variation of the results may also ensue from other methodological differences, e.g., differences in the sound intensity and duration, presentation of the sounds (headphones vs. loudspeaker), number of trials to be averaged, positioning of the subjects (seated vs. supine), time window

used for P50 identification, recognition of the P30 component, and measurement of the P50 amplitude (relative to the pre-stimulus baseline vs. preceding trough; see also Brockhaus-Dumke et al., 2008; de Wilde et al., 2007). As the present study is based on data obtained from patients with Alzheimer's disease, more research is needed to establish the generality of these results with healthy subjects (see also Chang et al., 2012) and other patient populations. It should also be accounted for that trains of four tones were used in this study, whereas a paired-click paradigm might yield different results. As a disadvantage of the present study may be mentioned the relatively small amount of trials (i.e., 40) to be included in the averages; increasing the amount of trials to, e.g., 200 might significantly improve the signal-to-noise ratio of the ERP waveforms without making the recording time too long for patients. Results may also be partly biased by artifacts as no rejection methods were used to exclude artifact-contaminated trials. In addition, the peak amplitudes may have been less biased by filters if measured relative to the preceding trough instead of the baseline (see also Widmann et al., 2015).

As a conclusion, filtering broadband signals, such as ERP waveforms, necessarily results in time-domain distortions. Thus, filters should not be used without careful consideration and not as a remedy for poor data quality, variability across subjects, or an inadequate number of trials to be averaged. A particular type of filter distortion may be acceptable for one experimental design, but lead to salient artificial effects in another. Instead of reusing filters applied in a previous study, the filter parameters need to be adjusted according to the ERP components under investigation. With thorough filter design it is possible to significantly improve the signal-to-noise ratio of the ERP waveforms and contribute to the importance of ERP research in cognitive neuroscience.

Acknowledgments

The authors are grateful to the staff of the Department of Clinical Neurophysiology in the Helsinki University Central Hospital, Jorvi Hospital for assistance with patient recordings; the authors particularly want to thank Nina Järvenpää, Matti Vartiainen, Sakari Jantunen, Pirkko Mäkinen, Marja-Liisa Vilmi, Maija Forsberg, and Ritva Tukiainen for their valuable work. The authors wish to express their gratitude to the Department of Neurology in the Helsinki University Central Hospital, Jorvi Hospital for enabling the patient recruitment. The authors wish to thank all the participants and their families whose participation made this study possible. The authors also wish to express their appreciation to Kirsi Palmu for her insightful comments and to Umesh Gowda and Tuomas Mutanen for MATLAB consultation during the preparation of this manuscript. The study was partly supported by the SalWe Research Program for Mind and Body (Tekes—the Finnish Funding Agency for Technology and Innovation grant 1104/10).

References

Acunzo, D.J., MacKenzie, G., van Rossum, M.C., 2012. Systematic biases in early ERP and ERF components as a result of high-pass filtering. J. Neurosci. Methods 209, 212–218, http://dx.doi.org/10.1016/j.jneumeth.2012.06.011.

Adler, L.E., Pachtman, E., Franks, R.D., Pecevich, M., Waldo, M.C., Freedman, R., 1982. Neurophysiological evidence for a defect in neuronal mechanisms involved in sensory gating in schizophrenia. Biol. Psychiatry 17, 639–654.

Ally, B.A., Jones, G.E., Cole, J.A., Budson, A.E., 2006. Sensory gating in patients with Alzheimer's disease and their biological children. Am. J. Alzheimers Dis. Other Dement. 21, 439–447, http://dx.doi.org/10.1177/1533317506292282.

American Psychiatric Association, 2000. Diagnostic and Statistical Manual of Mental Disorders. Text Rev., 4th ed. American Psychiatric Association, Washington, DC.

Başar, E., Rosen, B., Başar-Eroglu, C., Greitschus, F., 1987. The associations between 40Hz-EEG and the middle latency response of the auditory evoked potential. Int. J. Neurosci. 33, 103–117, http://dx.doi.org/10.3109/00207458708985933.

Boutros, N.N., Belger, A., 1999. Midlatency evoked potentials attenuation and augmentation reflect different aspects of sensory gating. Biol. Psychiatry 45, 917–922, http://dx.doi.org/10.1016/S0006-3223(98)00253-4.

Boutros, N.N., Korzyukov, O., Jansen, B., Feingold, A., Bell, M., 2004. Sensory gating deficits during the mid-latency phase of information processing in medicated schizophrenia patients. Psychiatry Res. 126, 203–215, http://dx.doi.org/10.1016/j.psychres.2004.01.007.

Braff, D.L., Geyer, M.A., 1990. Sensorimotor gating and schizophrenia. Human and animal model studies. Arch. Gen. Psychiatry 47, 181–188, http://dx.doi.org/10.1001/archpsyc.1990.01810140081011.

Brockhaus-Dumke, A., Mueller, R., Faigle, U., Klosterkoetter, J., 2008. Sensory gating revisited: relation between brain oscillations and auditory evoked potentials in schizophrenia. Schizophr. Res. 99, 238–249, http://dx.doi.org/10.1016/j.schres.2007.10.034.

Buchwald, J.S., Erwin, R.J., Read, S., Van Lancker, D., Cummings, J.L., 1989. Midlatency auditory evoked responses: differential abnormality of P1 in Alzheimer's disease. Electroencephalogr. Clin. Neurophysiol. 74, 378–384, http://dx.doi.org/10.1016/0168-5597(89)90005-1.

Cancelli, I., Cadore, I.P., Merlino, G., Valentinis, L., Moratti, U., Bergonzi, P., et al., 2006. Sensory gating deficit assessed by P50/Pb middle latency event related potential in Alzheimer's disease. J. Clin. Neurophysiol. 23, 421–425, http://dx.doi.org/10.1097/01.wnp.0000218991.99714.ee.

Chang, W.P., Gavin, W.J., Davies, P.L., 2012. Bandpass filter settings differentially affect measurement of P50 sensory gating in children and adults. Clin. Neurophysiol 123, 2264–2272, http://dx.doi.org/10.1016/j.clinph.2012.03.019.

Cohen, J., 1988. Statistical power analysis for the behavioral sciences, 2nd ed. Lawrence Erlbaum Associates, Hillsdale, NJ.

Cook, E.W., Miller, G.A., 1992. Digital filtering: background and tutorial for psychophysiologists. Psychophysiology 29, 350–367, http://dx.doi.org/10.1111/j.1469-8986.1992.tb01709.x.

Delorme, A., Makeig, S., 2004. EEGLAB: an open source toolbox for analysis of single-trial EEG dynamics including independent component analysis. J Neurosci Methods 134, 9–21, http://dx.doi.org/10.1016/j.jneumeth.2003.10.009.

de Wilde, O.M., Bour, L.J., Dingemans, P.M., Koelman, J.H., Linszen, D.H., 2007. A meta-analysis of P50 studies in patients with schizophrenia and relatives: differences in methodology between research groups. Schizophr Res 97, 137–151, http://dx.doi.org/10.1016/j.schres.2007.04.028.

Eccles, J.C., 1969. The inhibitory pathways of the central nervous system. Thomas, Springfield, IL.

Edgar, J.C., Stewart, J.L., Miller, G.A., 2005. Digital filters in ERP research. In: Handy, T.C. (Ed.), Event-related potentials: a methods handbook. MIT Press, Cambridge, MA, pp. 85–113.

Fein, G., Biggins, C., van Dyke, C., 1994. The auditory P50 response is normal in Alzheimer's disease when measured via a paired click paradigm. Electroencephalogr Clin Neurophysiol 92, 536–545, http://dx.doi.org/10.1016/0168-5597(94)90138-4.

Freedman, R., Waldo, M., Bickford-Wimer, P., Nagamoto, H., 1991. Elementary neuronal dysfunctions in schizophrenia. Schizophr Res 4, 233–243, http://dx.doi.org/10.1016/0920-9964(91)90035-P.

Freedman, R., Adler, L.E., Nagamoto, H.T., Waldo, M.C., 1998. Selection of digital filtering parameters and P50 amplitude. Biol Psychiatry 43, 921–922, http://dx.doi.org/10.1016/S0006-3223(98)00119-X.

Gmehlin, D., Kreisel, S.H., Bachmann, S., Weisbrod, M., Thomas, C., 2011. Age effects on preattentive and early attentive auditory processing of redundant stimuli: is sensory gating affected by physiological aging? J Gerontol A Biol Sci Med Sci 66, 1043–1053, http://dx.doi.org/10.1093/gerona/glr067.

Grunwald, T., Boutros, N.N., Pezer, N., von Oertzen, J., Fernandez, G., Schaller, C., et al., 2003. Neuronal substrates of sensory gating within the human brain. Biol Psychiatry 53, 511–519, http://dx.doi.org/10.1016/S0006-3223(02)01673-6.

Gustafsson, F., 1996. Determining the initial states in forward-backward filtering. IEEE Trans Signal Process 44, 988–992, http://dx.doi.org/10.1109/78.492552.

Jeong, J., 2004. EEG dynamics in patients with Alzheimer's disease. Clin Neurophysiol 115, 1490–1505, http://dx.doi.org/10.1016/j.clinph.2004.01.001.

Jerger, K., Biggins, C., Fein, G., 1992. P50 suppression is not affected by attentional manipulations. Biol Psychiatry 31, 365–377, http://dx.doi.org/10.1016/0006-3223(92)90230-W.

Jessen, F., Kucharski, C., Fries, T., Papassotiropoulos, A., Hoenig, K., Maier, W., et al., 2001. Sensory gating deficit expressed by a disturbed suppression of the P50 event-related potential in patients with Alzheimer's disease. Am J Psychiatry 158, 1319–1321, http://dx.doi.org/10.1176/appi.ajp.158.8.1319.

Kisley, M.A., Noecker, T.L., Guinther, P.M., 2004. Comparison of sensory gating to mismatch negativity and self-reported perceptual phenomena in healthy adults. Psychophysiology 41, 604–612, http://dx.doi.org/10.1111/j.1469-8986.2004.00191.x.

Light, G.A., Braff, D.L., 1998. The incredible shrinking P50 event-related potential. Biol Psychiatry 43, 918–920, http://dx.doi.org/10.1016/S0006-3223(98)00118-8.

Light, G.A., Braff, D.L., 1999. Human and animal studies of schizophrenia-related gating deficits. Curr Psychiatry Rep 1, 31–40, http://dx.doi.org/10.1007/s11920-999-0008-y.

Luck, S.J., 2005. An introduction to the event-related potential technique, 1st ed. MIT Press, Cambridge, MA.

Luck, S.J., 2014. An introduction to the event-related potential technique, 2nd ed. MIT Press, Cambridge, MA.

Mitra, S.K., 2011. Digital signal processing: a computer based approach, 4th ed. McGraw-Hill, New York, NY.
Mitra, P.P., Bokil, H., 2007. Observed brain dynamics. University Press, Oxford: Oxford.
Mullen, T., 2012. CleanLine EEGLAB plugin. Neuroimaging Informatics Tools and Resources Clearinghouse (NITRC), San Diego, CA.
Nitschke, J.B., Miller, G.A., Cook, E.W., 1998. Digital filtering in EEG/ERP analysis: some technical and empirical comparisons. Behav Res Methods Instrum Comput 30, 54–67, http://dx.doi.org/10.3758/BF03209416.
Parks, T.W., Burrus, C.S., 1987. Digital Filter Design. Wiley, New York, NY.
Patterson, J.V., Hetrick, W.P., Boutros, N.N., Jin, Y., Sandman, C., Stern, H., et al., 2008. P50 sensory gating ratios in schizophrenics and controls: a review and data analysis. Psychiatry Res 158, 226–247, http://dx.doi.org/10.1016/j.psychres.2007.02.009.
Picton, T.W., Bentin, S., Berg, P., Donchin, E., Hillyard, S.A., Johnson, R., et al., 2000. Guidelines for using human event-related potentials to study cognition: recording standards and publication criteria. Psychophysiology 37, 127–152, http://dx.doi.org/10.1111/1469-8986.3720127.
Picton, T.W., Lins, O.G., Scherg, M., 1995. The recording and analysis of event-related potentials. In: Boller, F., Grafman, J. (Eds.), Handbook of Neuropsychology. Elsevier Science B.V, Amsterdam, pp. 3–73.
Rousselet, G.A., 2012. Does filtering preclude us from studying ERP time-courses? Front Psychol 3, 131, http://dx.doi.org/10.3389/fpsyg.2012.00131.
Smith, D.A., Boutros, N.N., Schwarzkopf, S.B., 1994. Reliability of P50 auditory event-related potential indices of sensory gating. Psychophysiology 31, 495–502, http://dx.doi.org/10.1111/j.1469-8986.1994.tb01053.x.
Sörnmo, L., Laguna, P., 2005. Bioelectrical signal processing in cardiac and neurological applications. Elsevier Academic Press, Burlington, MA.
Tanner, D., Morgan-Short, K., Luck, S.J., 2015. How inappropriate high-pass filters can produce artifactual effects and incorrect conclusions in ERP studies of language and cognition. Psychophysiology 52, 997–1009, http://dx.doi.org/10.1111/psyp.12437.
Thomas, C., vom Berg, I., Rupp, A., Seidl, U., Schröder, J., Roesch-Ely, D., et al., 2010. P50 gating deficit in Alzheimer dementia correlates to frontal neuropsychological function. Neurobiol. Aging 31, 416–424, http://dx.doi.org/10.1016/j.neurobiolaging.2008.05.002.
Toyomaki, A., Hashimoto, N., Kako, Y., Tomimatsu, Y., Koyama, T., Kusumi, I., 2015. Different P50 sensory gating measures reflect different cognitive dysfunctions in schizophrenia. Schizophr. Res. 2, 166–169, http://dx.doi.org/10.1016/j.scog.2015.07.002.
VanRullen, R., 2011. Four common conceptual fallacies in mapping the time course of recognition. Front. Psychol. 2, 365, http://dx.doi.org/10.3389/fpsyg.2011.00365.
Wan, L., Friedman, B.H., Boutros, N.N., Crawford, H.J., 2008. P50 sensory gating and attentional performance. Int. J. Psychophysiol. 67, 91–100, http://dx.doi.org/10.1016/j.ijpsycho.2007.10.008.
Widmann, A., Schröger, E., 2012. Filter effects and filter artifacts in the analysis of electrophysiological data. Front. Psychol. 3, 233, http://dx.doi.org/10.3389/fpsyg.2012.00233.
Widmann, A., Schröger, E., Maess, B., 2015. Digital filter design for electrophysiological data—a practical approach. J. Neurosci. Methods 250, 34–46, http://dx.doi.org/10.1016/j.jneumeth.2014.08.002.
Yadon, C.A., Kisley, M.A., Davalos, D.B., 2015. The effects of vigilance and visual distraction on the P50 mid-latency auditory evoked potential. J. Psychophysiol. 29, 33–44, http://dx.doi.org/10.1027/0269-8803/a000132.
Yeung, N., Bogacz, R., Holroyd, C.B., Nieuwenhuis, S., Cohen, J.D., 2007. Theta phase resetting and the error-related negativity. Psychophysiology 44, 39–49, http://dx.doi.org/10.1111/j.1469-8986.2006.00482.x.